Neural Closed-loop Deep Brain Stimulation for Tremor Mitigation

Brady C. Houston

A dissertation submitted in
partial fulfillment of the
requirements for the degree of

Doctor of Philosophy

University of Washington

2017

Reading Committee:
Howard Chizeck, Chair
Andrew Ko
Steven Perlmutter
Rajesh Rao

Program authorized to offer degree:
Neuroscience

University of Washington

Abstract

Neural Closed-loop Deep Brain Stimulation for Tremor Mitigation

Brady C. Houston

Chair of the Supervisory Committee:
Professor Howard Chizeck
Electrical Engineering

Parkinson's disease and essential tremor are two common neurodegenerative disorders affecting millions of individuals. The hallmarks of these diseases are their interference with normal movement, which can greatly affect their sufferers' quality of life. Deep brain stimulation has emerged as therapy that can have a profound therapeutic effect on the symptoms of Parkinson's disease and essential tremor. Being a relatively new therapy, there is still much that can be done to optimize deep brain stimulation for clinical effect and device performance. Closed-loop stimulation, wherein stimulation is only given when the patient is experiencing symptoms, is a potential method for improving therapy. This closed-loop stimulation can be achieved using neural signals from the brains of Parkinson's and essential tremor patients to determine when they are experiencing symptoms.

This work describes the development and testing of a closed-loop DBS system for treating the symptoms of neurodegenerative movement disorders. First, the optimal neural signal source for a closed-loop system is investigated. After determining the optimal neural biofeedback signal, a closed-loop system is constructed that uses machine learning to build patient-specific models relating neural activity and tremor-inducing movements. This novel system is tested under various conditions, and is able to reliably deliver stimulation at the correct time and provide a highly therapeutic effect. This work serves as a proof-of-concept for the efficacy of machine-learning based, neural closed-loop deep brain stimulation systems for the treatment of neurodegenerative movement disorders.

Acknowledgments

There are many people without whom I never would have been able to complete this work. First and foremost, I want to thank my wife, Kate, for all of her support and love during this adventure. I also want to thank my parents and my wife's parents for their continued support of me and my family. I'm especially grateful for the example of my grandfather, who also finished his PhD in the pacific northwest, about 50 years ago.

I also want to thank my advisor, Howard Chizeck and my unofficial co-advisor, Andrew Ko, for all of their guidance and help. Similarly, this work would not have happened without the support of my fellow graduate students (in no particular order): Tim Brown, Andrew Haddock, Jeff Herron, Katherine Pratt and Maggie Thompson.

Contents

Chapter 1

Introduction

1.1 Background

Parkinson's disease and essential tremor are debilitating movement disorders. A common therapy for treating these diseases is deep brain stimulation. A description of these diseases, and deep brain stimulation as a treatment for them, is described in this section. Drawbacks to current methods for delivering deep brain stimulation, and closed-loop stimulation as a way to address these drawbacks, will also be expounded.

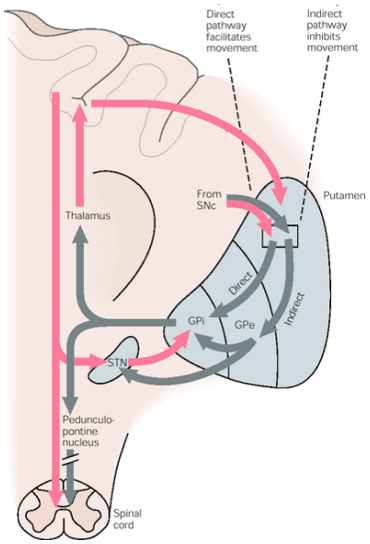

Figure 1.1: Schematic showing the thalamo-cortico-basal ganlia network. Excitatory connections are shown in red and inhibitory connections are shown in gray. The canonical direct and indirect pathways in the basal ganglia relay activity from the input nucleus of the basal ganglia, the putamen, into the output nucleus, the globus pallidus internus with differing effects. Taken from *Principles of Neural Science* [20].

1.1.1 Parkinson's Disease

Parkinson's disease (PD) occurs with a prevalence of approximately 0.3% of the entire population [23]. This prevalence is age-related, with about 1.0% of the population over 60 years old being affected, and even higher percentages at increasing ages [23]. It has been estimated that the total economic burden of PD in the United States is approximately 23 billion dollars, and that because of the aging population, this value will exceed 50 billion dollars by 2040 [40].

The symptomatic hallmarks of PD are mostly movement-related; they typically consist of bradykinesia (slow movement), postural instability, rigidity and rest tremor, although other

symptoms are also occasionally present [13]. At onset, symptoms of PD typically manifest in one limb, and then gradually spread to the rest of the body and worsen over time [13]. Rest tremor is typically the first symptom noticed by patients, and usually occurs at low frequencies from 2-7 Hz [29]. Needless to say, these symptoms can greatly impact normal activity and have a negative effect on the quality of life of those they effect [37].

PD is a neurodegenerative disease that is characterized by the loss of dopaminergic neurons in the substantia nigra pars compacta in the basal ganglia. These dopaminergic neurons project to the striatum and regulate activity in the two canonical basal ganglia pathways: the direct and indirect pathway (Figure 1.1). Due to the expression of different dopamine receptors, neurons projecting from the striatum to the globus pallidus externus (GPe) along the indirect pathway are inhibited by dopamine release, while neurons projecting to the globus pallidus internus (GPi) along the direct pathway are excited by dopamine release. Thus the death of dopaminergic neurons associated with PD is thought to have an overall effect of increasing activity in the indirect pathway and decreasing activity in the direct pathway, resulting in abnormal output into the thalamus and cortical motor areas [5][13]. Despite a thorough understanding of the pathophysiology of PD, its precise causes are still unknown. However, several environmental and genetic risk factors have been identified, and a combination of both is likely to cause the disease [13][23].

Although no therapy has been shown to reverse the progression of PD, treatment of symptoms caused by PD typically first consists of the administration of the dopamine precursor, L-DOPA. L-DOPA readily crosses the blood-brain barrier, where it is converted into dopamine by dopa-decarboxylase. Although initially effective in combating the symptoms of PD, eventually up to 60% of patients develop undesirable side effects related to the drug within 5 years [13]. When L-DOPA and other drugs are no longer therapeutically effective for managing symptoms, many PD patients undergo surgery for implantation of a deep brain stimulator (DBS) system (see section on DBS below).

1.1.2 Essential Tremor

Essential tremor (ET) is one of the most common neurological movement disorders, and occurs with a prevalence of approximately 4.5% of the population over the age of 65 [26]. Like PD, the occurence of ET is age-related, with prevalence increasing to close to 25% in the population over the age of 95 [26].

ET is most closely associated with kinetic (during intentional movement) and postural tremor [10]. Symptoms are most likely to be seen in upper limbs and the head, although tremor in other body areas also occurs [43]. Tremor typically occurs at frequencies between 3-12 Hz, and grows in amplitude over time [10]. At onset, tremor often begins in the dominant hand, but typically progresses into other body areas and worsens [31]. While ET has been called a "benign" disorder because it doesn't significantly reduce life expectancy, as does PD, it still can impair everday activities such as eating, writing and walking and thus have a large negative effect on quality of life [7][12].

Both the causes and pathophysiology of ET are not currently well understood. The pathophysiology of ET is thought to involve the degeneration of cerebellar Purkinje neurons and/or abnormal GABA signaling, and that these changes somehow influence the cerebellothalamacortical circuit to induce inappropriate network oscillations, leading to tremor [17][26]. However, how these phenomena arise and interact is not known. Similarly, the causes of ET are not understood, although like PD, there is evidence for both genetic and environmental risk factors [4].

As with PD, there are no current treatments that can reverse the damage already present in patients presenting with ET nor slow its progression. There are drugs that can ameliorate the tremor experienced by patients, such as beta-adrenergic receptor antagonists, but patients often become tolerant to these drugs [43]. When drugs are no longer a viable treatment option, invasive procedures such as thalamotomy or deep brain stimulator implantation are used with high success rates in alleviating tremor[43].

1.1.3 Deep Brain Stimulation

Deep brain stimulation (DBS) was first approved by the FDA as a therapy for the treatment of symptoms associated with the movement disorders Parkinson's disease and essential tremor in 1997. In the years since its approval, DBS has been safely implanted in many patients worldwide to treat these movement disorders with marked success. Since DBS requires invasive brain surgery and implants' finite lifespan can necessitate multiple procedures, it is often used as a last resort for those with intractable movement disorders who have ceased to respond to the administration of drugs such as L-DOPA (a dopamine precursor) for PD and beta blockers for ET.

A DBS system consists of an implanted pulse generator placed under the clavicle which

is connected to stimulating electrodes placed in deep brain structures. The most common anatomical targets of DBS are the internal globus pallidus (GPi) or subthalamic nucleus (STN) of the basal ganglia for treatment of PD and the ventral intermediate nucleus (VIM) of the thalamus for treatment of ET. These structures are critical parts of brain networks involved in movement, and their aberrant behavior has thus been implicated in movement disorders. Despite much research, the mechanism by which DBS in these areas alleviates the symptoms of movement disorders, such as rigidity, tremor and bradykinesia, is not greatly understood. It is generally thought that DBS overrides the abnormal neuronal activity in the brain regions in which it is implanted and facilitates non-pathological neuronal activity. This hypothesis has been supported by in-vivo recordings [28], as well as computation models [36].

Despite the concrete lack of understanding regarding the therapeutic mechanisms of DBS, the procedures for utilizing the technology have been well established. Currently, FDA-approved DBS electrodes typically have four annular contacts approximately 1.5 mm in length, spaced 0.5 mm apart (see Medtronic DBS lead, model 3389, for example). A single, biphasic pulse with a width of approximately 60-90 µs is delivered in a monopolar (one electrode contact acts as the cathode, and the metal case of the implanted DBS neurostimulator acts as the anode) or a bipolar (two contacts on the electrode) configuration [11]. These pulses are typically delivered at frequencies of 130-185 Hz and amplitudes of 0-6 Volts [11]. All of these parameters (pulse width, frequency and voltage) are fine-tuned by a clinician to optimize therapeutic effect while minimizing side effects.

While DBS provides invaluable therapeutic benefit for those suffering from these debilitating movement disorders, it is not without its shortfalls. DBS can cause undesired, stimulation-related side effects in both ET and PD patients. These side effects are typically related to the region into which the DBS electrode is implanted [11] and may be caused by sub-optimal electrode placement [3]. These stimulation-related side effects include dyskinesias (aberrant, uncontrolled movements), postural instability, speech dysfunction, tonic muscle contractions, paresthesia (numbness/tingling), eyelid and eye disturbances, and cognitive problems [11][43].

1.1.4 Current closed-loop technology and its drawbacks

As mentioned above, DBS consists of continuous, high-frequency stimulation delivered to various brain regions. This stimulation occurs at all times, regardless of the patient's symptoms and physical/mental state. Thus, despite its prevalent use and therapeutic efficacy, continuous

stimulation may not be the best paradigm for the treatment of dynamic movement disorders. Continuous stimulation can result in the side effects described above, unnecessarily deplete battery life (requiring surgery for replacement), require an onerous amount of clinician programming to find the best combination of parameters and may be a suboptimal therapy in general. In some cases, patients can use personal DBS programmers to change stimulation settings and/or disable/enable stimulation based on their desires, but in practice, at least anecdotally, this rarely occurs.

Recently, efforts have been made to improve DBS stimulation paradigms, namely by creating a closed-loop DBS system that is better suited to handle the dynamic nature of movement disorders. In such a system, a biofeedback signal is used to determine when a patient is experiencing symptoms and to what degree so that appropriate stimulation can be delivered (Figure 1.2). A closed-loop system would theoretically eliminate (or at least decrease) side effects created by unnecessary stimulation, decrease the clinician's burden in optimizing stimulation parameters and prolong battery life, lengthening the time in between procedures to replace the device's spent batteries or the device itself.

In this vein of research, several different types of biofeedback signals have been used to trigger stimulation or predict the presence of symptoms in human patients with movement disorders or non-human primates in disease models of movement disorders. These signals include: limb kinematics and muscle activity [8][9][14][42][19], neuronal action potentials from basal ganglia and cortex [34], and neural signals sensed from deep brain structures [25].

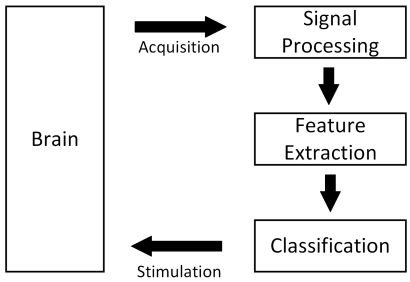

Figure 1.2: Block diagram depicting closed-loop DBS system using neural signals to trigger stimulation. Raw signals are recorded from the brain (either from deep brain structures or other areas) and are processed to remove stimulation artifacts, power line noise, etc. and isolate frequency bands of interest. Features that are correlated with symptoms are selected from the processed signals and inputted into a model which makes a prediction about whether symptoms are currently occurring (and possibly the severity of symptoms). The output of the model is then used to make a decision to alter stimulation parameters to abolish the symptoms.

Each of these signals sources have their benefits and drawbacks as they relate to closed-loop DBS. Limb kinematics and muscle activity are non-invasive and thus extremely safe signal sources that have activity that is highly correlated with movement, but they require patients to wear external devices that have to be donned/doffed and charged daily, and can serve as an uninvited reminder of their movement disorder.

Recording neural signals is typically more invasive, and high-quality neural signals require either implantation of additional electrodes, or using the DBS electrodes themselves. However, as these electrodes are implanted, they do not require the patient to deal with any external devices. It has been shown that neural signals can be reliably recorded from DBS electrodes despite large differences in stimulating and recording voltages [24], and it is well known that these neural signals are correlated with both normal and pathological movement (see section below). So, despite their invasive recording hardware, neural signals are a promising biofeedback signals for a closed-loop DBS system to treat movement disorders.

1.1.5 Neural Signals for Closed-Loop DBS

Neural signals that could potentially be used as a control signal for closed-loop DBS typically fall into two classes: those that sense single-unit activity (potentials from individual neurons), and those that sense aggregated activity from large groups or networks of neurons, typically referred to as local field potentials (LFPs). For DBS, the two main ways that field potentials can be acquired is through the DBS electrode itself or an additional electrocorticography (ECoG) electrode that rests on top of the cortex. Additionally, some studies have used non-invasive methods, such as electroencephalography (EEG) or magnetoencephalography (MEG) to study activity from large groups of neurons in the brains of patients with PD and ET. However, these methods would be impractical for closed-loop DBS, due to their need for large, complicated and expensive equipment.

While single-unit activity has been used in animal models for closed-loop DBS [34], the penetrating microelectrodes used for this type of recording are extremely invasive and typically do not provide long-lasting, reliable signals. LFPs, on the other hand, are less invasive, since they would either be sensed using electrodes that would be implanted anyway (DBS electrode), or an additional ECoG electrode that only rests on the surface of brain. Additionally, both PD and ET are thought to be diseases that affect networks of neurons (see PD and ET sections above), suggesting that LFPs may be a more appropriate signal than activity from single neurons. An important question regarding LFPs as signals for closed-loop DBS is how their activity correlates with the symptoms of the movement disorders that DBS is intended to treat.

There has been substantial research on characterizing LFPs from PD patients at the level of the basal ganglia. One of the most prominent spectral LFP features associated with PD is high oscillatory power in β-band (12-30 Hz) that is thought to correlate with the symptoms of

akinesia and bradykinesia [24]. This high β-band power is decreased by L-dopa administration and DBS in the STN, and β-band suppression has been correlated with motor improvement in PD patients [24]. It has also been shown that there is a suppression of β-band power just before the onset of tremor and during tremor in PD patients [41]. There are also changes in other frequency bands; there is increased coherence between muscle activity in limbs demonstrating tremor and STN LFP in the tremor band (4-7 Hz) and double the tremor band (10-14 Hz) during tremor [33]. Changes in spectral power in PD have also been found in higher frequencies; L-Dopa administration has been shown to change the spectral power in the STN at frequencies of 250 and 350 Hz [30] and increase power in the gamma band (30-100 Hz) in the STN [6].

All the studies above have focused on neural activity in deep brain nuclei in the basal ganglia. As mentioned above, cortical activity is also a potential signal source for closed-loop DBS. Several studies have shown changes in cortical field potential $\beta-$band power in PD that was modulated by DBS and administration of L-dopa using EEG and MEG [39][38]. Studies using ECoG to examine cortical activity in PD have shown decreases in β-band power during rest tremor [32], as well as changes in higher-order spectral phenomenon, such as phase-amplitude coupling [18]. When taken together, these studies characterizing LFPs in deep brain structures and cortical areas demonstrate that the symptoms of PD are associated with changes in oscillatory activity in much of the LFP spectrum. This suggests that neural features from field potentials may be useful in detecting PD symptoms in a closed-loop system.

Studies seeking to characterize changes in LFP activity associated with ET are not as extensive as those involving PD, but some changes in LFP features have been associated with ET. The most prominent changes in LFPs are concentrated to low frequences; ET is associated with increased power in the tremor frequency band (4-12 Hz) when compared to patients with other disorders (multiple sclerosis, chronic pain) [21]. Coherence between limbs showing tremor and neural signals is also prominent in ET; there is significant coherence between muscle activity in limbs showing tremor and LFP activity in the VIM at tremor frequencies [21][27] and coherence at the same frequencies between limb tremor activity and EEG signals [16][27]. $\beta-$band power is also inversely related to tremor band amplitude [2][15]. Using electrocorticography, DBS has been shown to decrease activity in $\alpha-$band (8-12 Hz) in primary motor cortex and $\theta-$band (4-8 Hz) in primary somatosensory cortex [1]. While it can be difficult to parse out whether the effects on cortical LFP activity stem from movement or tremor itself, several studies have shown that movement elicits decreases in $\beta-$band power in ET [22][35]. Because tremor is induced by

movement in ET, it may not be necessary for a closed-loop system to actually detect tremor in order to be useful; rather, it could just deliver stimulation whenever tremor-inducing movement is detected. So, like LFP phenomena in PD, these studies suggest that LFP features will be predictive of the presence of tremor-inducing movements in ET patients and thus useful in a closed-loop DBS system.

1.2 Specific Aims

Aim 1: Determine to what extent Parkinsonian and essential tremor can be detected from chronically-implanted DBS electrodes

As described above, both the symptoms of PD and ET appear to be correlated with consistent changes in LFP activity at the level of deep brain nuclei. There have also been several studies that have used machine learning algorithms to examine how well Parkinsonian tremor can be detected from deep brain activity (see Chapter 2). However, these studies have only used data recorded intra-operatively and analyzed offline, and all have only used data from PD patients. Intra-operative studies, while useful for characterizing neural activity, typically use high-performance, yet cumbersome recording hardware. It is therefore unknown how well Parkinsonian and essential tremor can be detected using signals recorded from commercially-available (if currently investigational), chronically-implanted DBS hardware. Therefore, for this aim, I used machine learning to build subject-specific models to detect tremor offline using neural activity recorded from deep brain nuclei in both ET and PD subjects implanted with chronic DBS systems.

Aim 2: Determine to what extent essential tremor can be detected from chronically-implanted cortical electrodes

Aim 1 elucidated how well deep brain signals could be used to detect tremor in PD and ET subjects. Again, as in aim 1, symptom-related changes in cortical LFPs have been characterized using intra-operative data. However, actual tremor-inducing movement detection from LFPs has not been investigated, nor has detection using chronically-implanted cortical electrodes. Aim 1 afforded algorithms that could be used to examine tremor-inducing movement detection using signals recorded from deep brain nuclei, and these algorithms are readily extendable for use with cortical signals. Therefore, for this aim, neural activity was recorded from the cortex of

ET subjects during tremor-inducing movement and used to quantify how well tremor-inducing movement could be detected. Again, movement detection was accomplished using chronically-implanted ECoG electrodes. This detection was compared to detection using deep brain signals to determine which is best for use in a closed-loop DBS system.

Aim 3: Develop and test the performance of a neural biofeedback signal, closed-loop system for mitigating essential tremor

Aims 1 and 2 provided valuable information on how well tremor-inducing movement could be detected offline using data recorded during tremor-inducing movement and rest. The offline performance of models for tremor detection is a good indication of how well classifiers would perform online, and thus informed which of the two signal sources is likely to work best in an actual closed-loop DBS system. This information was used to build a closed-loop DBS system using one of the signal sources that could detect tremor-inducing movement and change stimulation parameters in real time. This system was tested in several ET subjects and its performance, both in terms of tremor-inducing movement detection and therapeutic effect, was examined.

References

[1] E. L. Air, E. Ryapolova-Webb, C. de Hemptinne, J. L. Ostrem, N. B. Galifianakis, P. S. Larson, E. F. Chang, and P. a. Starr, "Acute effects of thalamic deep brain stimulation and thalamotomy on sensorimotor cortex local field potentials in essential tremor.," *Clinical neurophysiology : official journal of the International Federation of Clinical Neurophysiology*, vol. 123, no. 11, pp. 2232–8, 2012.

[2] D. Basha, J. O. Dostrovsky, A. L. Lopez Rios, M. Hodaie, A. M. Lozano, and W. D. Hutchison, "Beta oscillatory neurons in the motor thalamus of movement disorder and pain patients.," *Experimental neurology*, vol. 261, pp. 782–790, Sep. 2014.

[3] A. L. Benabid, S. Chabardes, J. Mitrofanis, and P. Pollak, "Deep brain stimulation of the subthalamic nucleus for the treatment of Parkinson's disease," *The Lancet Neurology*, vol. 8, no. 1, pp. 67–81, 2009.

[4] J. Benito-León and E. D. Louis, "Essential tremor: emerging views of a common disorder.," *Nature clinical practice. Neurology*, vol. 2, no. 12, 666–78, quiz 2p following 691, 2006.

[5] J.-S. Brittain and P. Brown, "Oscillations and the basal ganglia: motor control and beyond.," *NeuroImage*, vol. 85 Pt 2, pp. 637–47, 2014.

[6] P. Brown, A. Oliviero, P. Mazzone, A. Insola, P. Tonali, and V. D. Lazzaro, "Dopamine Dependency of Oscillations between Subthalamic Nucleus and Pallidum in Parkinson ' s Disease," *Journal of Neuroscience*, vol. 21, no. 3, pp. 1033–1038, 2001.

[7] K. L. Busenbark, J. Nash, S. Nash, J. P. Hubble, and W. C. Koller, "Is essential tremor benign?" *Neurology*, vol. 41, no. 12, p. 1982, 1991.

[8] H. Cagnan, J.-S. Brittain, S. Little, T. Foltynie, P. Limousin, L. Zrinzo, M. Hariz, C. Joint, J. Fitzgerald, A. L. Green, T. Aziz, and P. Brown, "Phase dependent modulation of tremor amplitude in essential tremor through thalamic stimulation.," *Brain : a journal of neurology*, vol. 136, no. Pt 10, pp. 3062–75, 2013.

[9] H. Cagnan, D. Pedrosa, S. Little, A. Pogosyan, B. Cheeran, T. Aziz, A. Green, J. Fitzgerald, T. Foltynie, P. Limousin, L. Zrinzo, M. Hariz, K. J. Friston, T. Denison, and P. Brown, "Stimulating at the right time: phase-specific deep brain stimulation," *Brain*, no. 2016, pp. 1–14, 2016.

[10] G. Deuschl, P. Bain, and M. Brin, "Consensus statement of the movement disorder society on tremor," *Movement Disorders*, vol. 13, no. S3, pp. 2–23, 1998.

[11] G. Deuschl, J. Herzog, G. Kleiner-Fisman, C. Kubu, A. M. Lozano, K. E. Lyons, M. C. Rodriguez-Oroz, F. Tamma, A. I. Tröster, J. L. Vitek, J. Volkmann, and V. Voon, "Deep brain stimulation: Postoperative issues," *Movement Disorders*, vol. 21, no. SUPPL. 14, 2006.

[12] A. Diamond and J. Jankovic, "The effect of deep brain stimulation on quality of life in movement disorders.," *Journal of neurology, neurosurgery, and psychiatry*, vol. 76, no. 9, pp. 1188–93, 2005.

[13] S. Fahn, "Description of parkinson's disease as a clinical syndrome," *Annals of the New York Academy of Sciences*, vol. 991, no. 1, pp. 1–14, 2003.

[14] D. Graupe, I. Basu, D. Tuninetti, P. Vannemreddy, and K. V. Slavin, "Adaptively controlling deep brain stimulation in essential tremor patient via surface electromyography.," *Neurological research*, vol. 32, no. 9, pp. 899–904, Nov. 2010.

[15] D. M. Halliday, B. a. Conway, S. F. Farmer, U. Shahani, a. J. Russell, and J. R. Rosenberg, "Coherence between low-frequency activation of the motor cortex and tremor in patients with essential tremor.," *Lancet*, vol. 355, no. 9210, pp. 1149–53, 2000.

[16] B. Hellwig, S. Häußler, B. Schelter, M. Lauk, B. Guschlbauer, J. Timmer, and C. H. Lücking, "Early report Tremor-correlated cortical activity in essential tremor," *Lancet*, vol. 357, pp. 519–523, 2001.

[17] R. C. Helmich, I. Toni, G. Deuschl, and B. R. Bloem, "The pathophysiology of essential tremor and parkinson's tremor," *Current Neurology and Neuroscience Reports*, vol. 13, no. 9, 2013.

[18] C. de Hemptinne, E. S. Ryapolova-Webb, E. L. Air, P. a. Garcia, K. J. Miller, J. G. Ojemann, J. L. Ostrem, N. B. Galifianakis, and P. a. Starr, "Exaggerated phase-amplitude coupling in the primary motor cortex in Parkinson disease.," *Proceedings of the National Academy of Sciences of the United States of America*, vol. 110, no. 12, pp. 4780–5, 2013.

[19] J. A. Herron, M. C. Thompson, T. Brown, H. J. Chizeck, J. G. Ojemann, and A. L. Ko, "Chronic electrocorticography for sensing movement intention and closed-loop deep brain stimulation with wearable sensors in an essential tremor patient," *Journal of Neurosurgery*, pp. 1–8, 2016.

[20] E. R. Kandel, J. H. Schwartz, T. M. Jessell, S. A. Siegelbaum, and A. J. Hudspeth, *Principles of neural science*. McGraw-hill New York, 2000, vol. 4.

[21] A. Kane, W. D. Hutchison, M. Hodaie, A. M. Lozano, and J. O. Dostrovsky, "Enhanced synchronization of thalamic theta band local field potentials in patients with essential tremor.," *Experimental neurology*, vol. 217, no. 1, pp. 171–6, 2009.

[22] E. D. Kondylis, M. J. Randazzo, A. Alhourani, W. J. Lipski, T. A. Wozny, Y. Pandya, A. S. Ghuman, R. S. Turner, D. J. Crammond, and R. M. Richardson, "Movement-related dynamics of cortical oscillations in Parkinson ' s disease and essential tremor," pp. 1–13, 2016.

[23] L. M. de Lau and M. M. Breteler, "Epidemiology of parkinson's disease," *The Lancet Neurology*, vol. 5, no. 6, pp. 525–535, 2006.

[24] S. Little and P. Brown, "What brain signals are suitable for feedback control of deep brain stimulation in Parkinson's disease?" *Annals of the New York Academy of Sciences*, vol. 1265, pp. 9–24, 2012.

[25] S. Little, A. Pogosyan, S. Neal, B. Zavala, L. Zrinzo, M. Hariz, T. Foltynie, P. Limousin, K. Ashkan, J. FitzGerald, A. L. Green, T. Z. Aziz, and P. Brown, "Adaptive deep brain stimulation in advanced Parkinson disease.," *Annals of neurology*, vol. 74, no. 3, pp. 449–57, 2013.

[26] E. D. Louis and J. J. Ferreira, "How common is the most common adult movement disorder? update on the worldwide prevalence of essential tremor," *Movement Disorders*, vol. 25, no. 5, pp. 534–541, 2010.

[27] J. F. Marsden, P. Ashby, P. Limousin-Dowsey, J. C. Rothwell, and P. Brown, "Coherence between cerebellar thalamus, cortex and muscle in man: cerebellar thalamus interactions.," *Brain : a journal of neurology*, vol. 123 (Pt 7, pp. 1459–70, Jul. 2000.

[28] S. Miocinovic, S. Somayajula, S. Chitnis, and J. L. Vitek, "History, applications, and mechanisms of deep brain stimulation.," *JAMA neurology*, vol. 70, no. 2, pp. 163–71, Feb. 2013.

[29] P. E. O'Suilleabhain and J. Y. Matsumoto, "Time-frequency analysis of tremors.," *Brain : a journal of neurology*, vol. 121 (Pt 1, pp. 2127–34, 1998.

[30] T. E. Özkurt, M. Butz, M. Homburger, S. Elben, J. Vesper, L. Wojtecki, and A. Schnitzler, "High frequency oscillations in the subthalamic nucleus: a neurophysiological marker of the motor state in Parkinson's disease.," *Experimental neurology*, vol. 229, no. 2, pp. 324–31, 2011.

[31] J. D. Putzke, N. R. Whaley, Y. Baba, Z. K. Wszolek, and R. J. Uitti, "Essential tremor: predictors of disease progression in a clinical cohort.," *Journal of neurology, neurosurgery, and psychiatry*, vol. 77, no. 11, pp. 1235–1237, 2006.

[32] S. E. Qasim, C. de Hemptinne, N. C. Swann, S. Miocinovic, J. L. Ostrem, and P. A. Starr, "Electrocorticography reveals beta desynchronization in the basal ganglia-cortical loop during rest tremor in Parkinson's disease," *Neurobiology of Disease*, vol. 86, pp. 177–186, 2015.

[33] C. Reck, E. Florin, L. Wojtecki, H. Krause, S. Groiss, J. Voges, M. Maarouf, V. Sturm, A. Schnitzler, and L. Timmermann, "Characterisation of tremor-associated local field potentials in the subthalamic nucleus in Parkinson's disease.," *The European journal of neuroscience*, vol. 29, no. 3, pp. 599–612, Mar. 2009.

[34] B. Rosin, M. Slovik, R. Mitelman, M. Rivlin-Etzion, S. N. Haber, Z. Israel, E. Vaadia, and H. Bergman, "Closed-loop deep brain stimulation is superior in ameliorating parkinsonism.," *Neuron*, vol. 72, no. 2, pp. 370–84, 2011.

[35] N. C. Rowland, C. D. Hemptinne, N. C. Swann, S. Qasim, S. Miocinovic, J. L. Ostrem, R. T. Knight, and P. A. Starr, "Task-related activity in sensorimotor cortex in Parkinson ' s disease and essential tremor : changes in beta and gamma bands," *Frontiers in Human Neuroscience*, vol. 9, no. September, pp. 1–12, 2015.

[36] J. E. Rubin and D. Terman, "High frequency stimulation of the subthalamic nucleus eliminates pathological thalamic rhythmicity in a computational model.," *Journal of computational neuroscience*, vol. 16, no. 3, pp. 211–35, 2004.

[37] A. Schrag, M. Jahanshahi, and N. Quinn, "What contributes to quality of life in patients with parkinson's disease?" *Journal of Neurology, Neurosurgery and Psychiatry*, vol. 69, no. 3, pp. 308–312, 2000.

[38] P. Silberstein, A. Pogosyan, A. a. Kühn, G. Hotton, S. Tisch, A. Kupsch, P. Dowsey-Limousin, M. I. Hariz, and P. Brown, "Cortico-cortical coupling in Parkinson's disease and its modulation by therapy.," *Brain : a journal of neurology*, vol. 128, no. Pt 6, pp. 1277–91, 2005.

[39] D. Stoffers, J. L. W. Bosboom, J. B. Deijen, E. C. Wolters, C. J. Stam, and H. W. Berendse, "Increased cortico-cortical functional connectivity in early-stage Parkinson's disease: an MEG study.," *NeuroImage*, vol. 41, no. 2, pp. 212–22, 2008.

[40] "The economic impact of parkinson's disease," *Parkinsonism and Related Disorders*, vol. 13, Supplement, S8–S12, 2007.

[41] S. Wang, Y. Chen, M. Ding, J. Feng, J. Stein, T. Aziz, and X. Liu, "Revealing the dynamic causal interdependence between neural and muscular signals in Parkinsonian tremor," *Journal of the Franklin Institute*, vol. 344, no. 3-4, pp. 180–195, May 2007.

[42] T. Yamamoto, Y. Katayama, J. Ushiba, H. Yoshino, T. Obuchi, K. Kobayashi, H. Oshima, and C. Fukaya, "On-demand control system for deep brain stimulation for treatment of intention tremor.," *Neuromodulation : journal of the International Neuromodulation Society*, vol. 16, no. 3, 230–5, discussion 235, 2013.

[43] T. A. Zesiewicz, R. Elble, E. D. Louis, W. G. Ondo, G. S. Gronseth, and W. J. Weiner, "Practice Parameter : Therapies for essential tremor Report of the Quality Standards Subcommittee of the," 2005.

Chapter 2

Offline Tremor Detection From DBS Electrodes

2.1 Introduction

This chapter presents work done to address aim 1 of this dissertation: **determine to what extent Parkinsonian and essential tremor can be detected from chronically-implanted DBS electrodes.**

Successful CLDBS could theoretically be developed using at least one of two different classes of biosignals to indicate when tremor is occurring. These classes are I. signals generated from actual movement (e.g. inertial measurements, muscle activity) or II. neural signals. While movement is readily detected from accelerometers, gyroscopes and/or EMG, these signals all require the user to wear an external device for functionality. Dependence on such devices can be an annoyance for users, and can also serve as an unwelcome reminder of their disease and the implanted system. Neural signals, on the other hand, can be recorded from already implanted DBS systems, therefore removing the need for any other device in the loop. Another downside to signals stemming from actual movement is their latency; delays between neural signals preceding and accompanying the onset of movement can be on the order of a hundred or more milliseconds. Using neural signals themselves can avoid this delay in the system.

The most accessible neural signal for current DBS technology is local field potentials (LFP) sensed from contacts on the actual DBS electrode itself. In order for these neural signals to be of utility in a CLDBS system for mitigating tremor, they must reliably show activity that correlates with tremor, or tremor-inducing movement, in such a way that mathematical models

can be constructed relating the two. Previous studies have shown that tremor is accompanied by several changes in neural signals from DBS electrodes. In PD, Reck, et al, found that there were peaks in LFP spectra at the frequency of tremor and double the frequency of tremor in recordings from STN [12]. It has also been shown that there is beta-band suppression preceding the onset of tremor [17], and that beta-band is suppressed during tremor and re-emerges after its cessation in the STN [4]. Tass, et al, confirmed that both STN tremor-band and STN beta-band oscillations contribute to tremor [16]. In essential tremor, Basha, et al, showed that tremor is accompanied by beta-band suppression in the VIM [3].

While these gross features in neural signals are present during tremor, patient-specific nuances in these signals may make using these gross features (such as beta-band power) across all patients difficult. Manually examining signals from each patient to discover these nuances would be far too onerous for practical usage, so several studies have used machine learning algorithms to determine optimal features for detecting symptoms in individual patients [2][1][7][10][18]. All of these studies used LFPs recorded from STN electrodes to detect Parkinsonian tremor.

However, in all of these tremor-detection studies, neural signals were recorded intra- and perioperatively. After implantation of the device, it is possible for signal fidelity to be diminished. This could possibly occur from foreign body response to the electrode, including encapsulation, or shifting of the electrode. It is not known whether these occurrences compromise the utility of neural signals recorded from the electrode to detect tremor. Furthermore, these events can happen over the course of months to years. Coupled with the neurodegenerative nature of movement disorders, it is unknown whether tremor can be robustly detected from these neural signals over extended periods of time, and whether they can be detected at all using signals from the DBS electrode in ET patients. To address these questions, I used data recorded from chronically-implanted DBS systems in subjects with PD and ET. Using these data, classifiers were trained and tested offline to detect tremor or tremor-inducing movement.

2.2 Methods

2.2.1 Data Collection

All experiments were approved by the FDA (IDE received) and the Stanford University or University of Washington IRB committee, and the patients gave informed consent. The data for this study were collected from seven subjects who had been diagnosed with tremor-dominant

PD and two subjects who had been diagnosed with ET. All subjects had been implanted with the Medtronic Activa PC+S® DBS system, with the DBS electrode implanted in the STN (unilateral or bilateral) for PD subjects and in the VIM (unilateral) of the thalamus for ET subjects. Additionally, both ET subjects had a four-contact electrocorticography (ECoG) electrode implanted over the hand/arm region of M1/S1 (the work of this chapter will focus solely on signals recorded from the DBS electrode for both patient populations). Around one month after implantation, each subjects' DBS system was programmed for optimal therapeutic effect. Thereafter, subjects returned for follow-up visits every one to three months to optimize the stimulation parameters. Because of the ability of the Activa PC+S® system to record LFPs from the stimulating electrodes and transmit the data for offline analysis, we obtained neural data from each subject during these follow-up visits.

For PD subjects, during each visit, data were recorded while the subject was at rest in sitting, lying and standing positions. There were typically between 3-5 minutes of total recorded data for each subject for each visit, and tremor was present in at least one position (see Figure 2.1, top panel, for an example of movement data recorded from a visit). Movement activity was recorded by a solid-state gyroscopic sensor sampled at 1000 Hz from upper and lower extremities for monitoring tremor during the resting task. Upper limb EMG data and synchronized video were also collected during the task and used to confirm that the periods of interest contained no voluntary movement. LFPs were recorded from STN DBS lead onto the Activa PC+S® neurostimulator. As the DBS lead was implanted so that the deepest contact (0) was at the base of the STN, recordings were made using contacts 2-0, unless there was significant ECG leakage on those contacts. In that case, contacts 3-1 were used for recording. Pre-amplified STN LFP signals were high-pass filtered at 0.5 Hz and low-pass filtered at 100 Hz. All LFP data were sampled at 422 Hz (10-bit resolution) with a gain of 2000. Uncompressed LFP was extracted via telemetry and transferred to a computer for offline analysis. At the start of every recording, a brief 20 Hz/1 V stimulation was delivered so that sensing hardware could be synced but afterwards no stimulation was delivered during the remainder of the task. All subjects were in an OFF-medication state during the task.

For ET subjects, during each visit, neural data were recorded while the subject engaged in prompted movement tasks. Specific movements were different for the two subjects because different movements evoked tremor. However, both subjects performed prompted movements using their right arm and hand while in a sitting position. Movements typically lasted 10-30

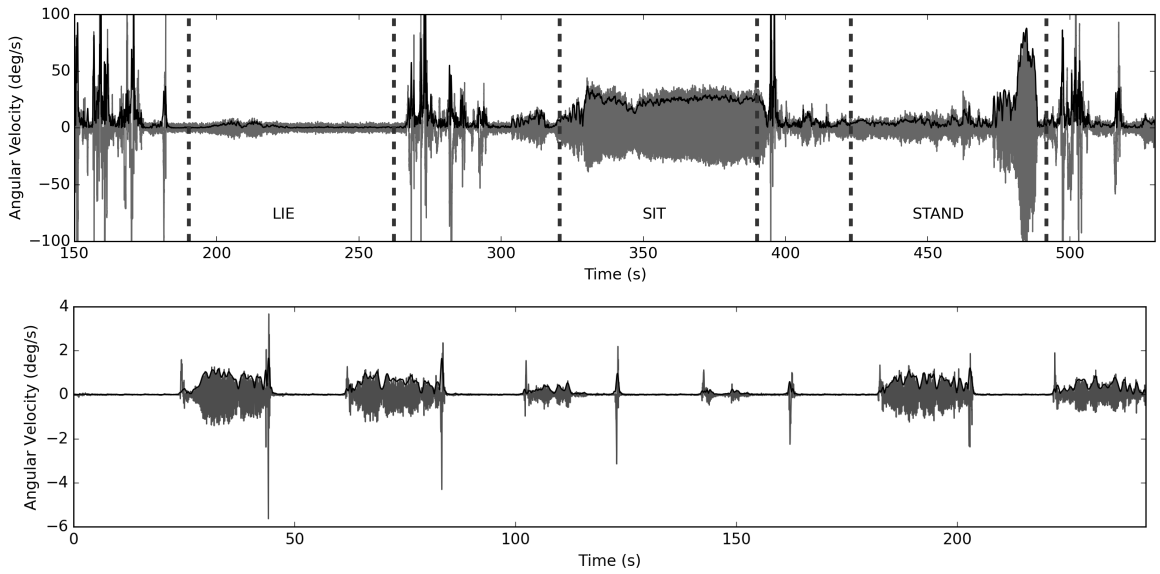

Figure 2.1: Top panel: Example of gyroscopic movement data recorded from tremoring limb of a subject with PD during standing, sitting and lying periods (gray) and instantaneous tremor amplitude (black). Dashed gray lines demarcate the beginning and end of the indicated position. Bottom panel: gyroscopic movement data recorded from the right arm of a subject with ET (gray) with instantaneous tremor amplitude (black). Prompted movement periods of approximately 30 seconds are interspersed with rest periods of the same duration.

seconds, and were interspersed with rest periods of a similar duration. In total, 3-4 minutes of data were recorded during the task. Movement activity was recorded using the onboard IMU of a consumer smartwatch, worn on the subject's wrist. Accelerometer, gyroscope and magnetometer data were sampled at 100 Hz. See 2.1, bottom panel, for an example of movement data collected during the task.

During the prompted movement task, LFP data were streamed in real time from the VIM DBS lead onto a laptop computer. For ET subject S1, contacts 3-0 were used for recording and for ET subject S2, contacts 3-1 were used for recording. Neural signals were were high-pass filtered at 0.5 Hz and low-pass filtered at 100 Hz. All LFP data were sampled at 422 Hz (10-bit resolution) with a gain of 2000. Subject S1 was in an OFF-medication state during the task, but subject S2 was taking propranolol (beta-blocker) and primidone (anti-convulsant) for treatment of ET.

2.2.2 Data Processing

For PD subjects, movement data from the limb most affected by tremor were first downsampled to 422 Hz and then filtered in both directions by a 4^{th}-order butterworth bandpass filter. The Hilbert transform was then used to find the instantaneous amplitude of the peak tremor

frequency in the movement data (Fig. 2.1, top panel). The instantaneous tremor amplitude was then thresholded at 10 deg/s to label tremor and tremor-free periods. For ET subjects, movement data from the affected limb were visually inspected to determine periods containing prompted movement and periods free from movement.

To examine differences in neural activity across PD subjects during tremor and when absent from tremor, all data from each subject were examined to find periods of 30 seconds or more that could be labeled as tremor or tremor-free as unequivocally as possible (i.e. large tremor amplitude and very-low/absent tremor amplitude). This yielded between 1 and 6 periods of tremor and tremor-free recordings for each subject, depending on the nature of their tremor and their number of visits, that were used for spectral analysis. From these tremor and tremor-free periods, "best" and "averaged" tremor and tremor-free spectra for each of the seven subjects were calculated. "Best" tremor and tremor-free spectra were calculated from the 30 seconds of neural recordings from each subject that had the highest and lowest average tremor amplitude, respectively. "Averaged" tremor and tremor-free spectra for each subject were calculated from all the data selected for spectral analysis for that subject. Power spectral density was calculated using Welch's method with a 5-second Hann window and 50% overlap (for "averaged" spectra, PSD for each period was calculated using Welch's method, then averaged together). Log power was averaged over the following five frequency ranges to examine differences between spectra: alpha (4-8 Hz), theta (8-12 Hz), low beta (12-20 Hz), high beta (20-30 Hz) and low gamma (30-50 Hz). Significant differences across the population were tested using the Wilcoxon signed-rank test if a k-test detected a non-normal distribution, otherwise a paired t-test was used. Benjamini-hochberg corrections were used for multiple comparisons.

To examine differences in neural activity during rest and movement in ET subjects, PSD was estimated for each movement and rest period (approximately 4-7 20-30 second periods for each) using Welch's method with a Hann window length of 5 seconds with 50% overlap. Log power was averaged over the same bins described in the previous paragraph. Because of the small number of ET subjects, only differences between spectra within individual subjects were examined. Significant differences within subjects were tested using the Mann-Whitney-U test if a k-test detected a non-normal distribution, otherwise a t-test was used. Benjamini-hochberg corrections were used for multiple comparisons.

2.2.3 Classifier Training/Testing

Neural features for building classifiers for tremor detection were extracted from STN (PD) or VIM (ET) by chunking the LFP data into overlapping windows every 200 ms (the window length was varied between 1 and 5 seconds to examine the effect of window length on classifier performance). Each of these chunks had its power spectral density (PSD) estimated using Welch's method with a 1-second Hann window and 50% overlap. Differences in PSD between tremor and tremor-free epochs were largely contained between 4-30 Hz, so PSD in approximately 1 Hz bins in this range was then used as features for the training and testing of a binary classifier. Each of the LFP chunks was labeled as tremor or tremor-free using the thresholded instantaneous tremor amplitude data for PD subjects or the visually inspected movement data for ET subjects.

For all ET and PD subjects, LFP features and their corresponding labels were divided equally into two sets with approximately equal proportions of tremor (or tremor-inducing movement) and tremor-free recordings using all the data from each subject's visit (visits which had insufficient tremor and tremor-free periods were excluded) for PD subjects, or the entire prompted movement task for ET subjects. Each of the two data sets for a subject was used to train a classifier. To prevent overfitting, L_2-norm regularization was used, and the optimal regularization hyperparameter was selected using 2-fold cross-validation. The classifier was optimized using standard gradient descent methods for either accuracy or sensitivity (true positive rate, recall) to examine the effect of optimizing for different metrics. For reference, the formulas for accuracy and sensitivity, respectively, are

$$\text{Accuracy} = \frac{TP + TN}{TP + TN + FP + FN}, \quad \text{Sensitivity} = \frac{TP}{TP + FN}$$

where TP is true positive, TN is true negative, FN is false negative, FP is false positive (true/false is relative to ground truth, positive/negative is output from classifier; e.g. true positive is tremor is actually occurring and detector predicts that tremor is occurring). All metrics are therefore "cross-validation" scores, rather than "testing" scores, and are reported as the average for the two classifiers. Each feature (PSD in 1 Hz bins between 4 or 5 and 30 Hz) from the training set was normalized to have zero mean and unit variance and then used to train a regularized logistic regression classifier. The testing set was normalized by the mean and variance of the training set, and then the label for each chunk was predicted using

the trained classifier. Performance of the classifier was measured with accuracy and sensitivity using the instantaneous tremor amplitude data for ground truth. Above-chance performance was determined using McNemar's test.

To examine long-term detection of tremor in PD, LFP features from an entire visit were used to train the classifier. Features were extracted in the same manner as described in the previous paragraphs, and two-fold cross-validation was used to select the optimal hyperparameter for regularization (again optimizing individually for accuracy and sensitivity). However, after selecting the optimal hyperparameter, the classifier was re-trained using all the data from the visit. After training, the classifier was used to detect tremor in all subsequent visits. Out of the seven subjects, only three had more than two visits and thus only their data were used for this analysis.

2.3 Results

2.3.1 Parkinson's Disease

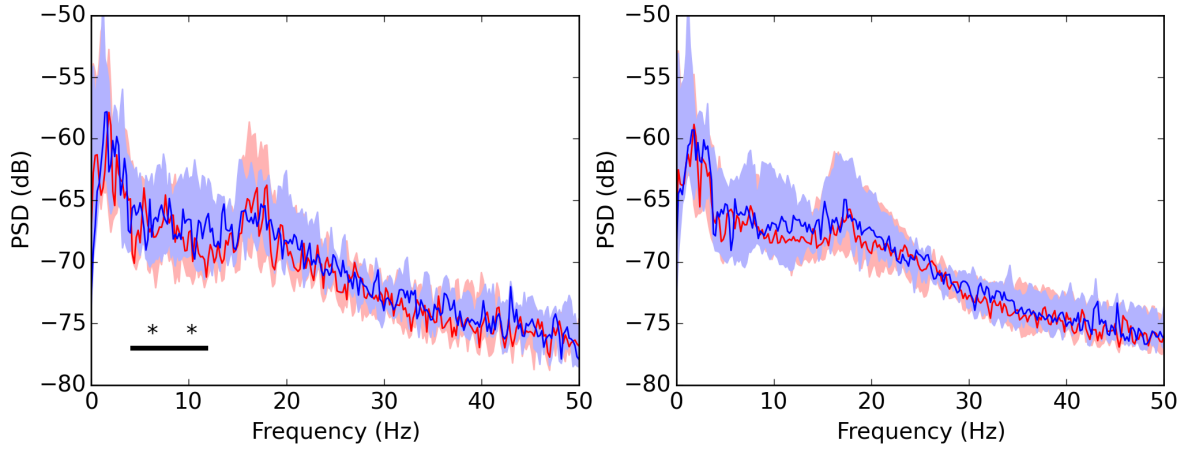

Figure 2.2: LFP spectra during tremor (red) and tremor-free (blue) periods in PD subjects (n = 7). **Left panel:** Data are from the single 30-second period that has the highest and lowest average tremor amplitude (for tremor and tremor-free spectra, respectively) and are shown as median and interquartile range. There was a significant difference in theta (4-8 Hz) and alpha (8-12 Hz) bands between tremor and tremor-free PSD. **Right panel:** Data are from all the tremor and tremor-free periods selected for spectral analysis (1-6 periods for each patient for both tremor and tremor-free recordings). After averaging each subject's periods together, significant differences disappear.

The work presented in this chapter aims to answer the question: **to what extent can Parkinsonian and essential tremor be detected from chronically-implanted DBS electrodes?** To answer this question for Parkinsonian tremor, I first examined spectra from STN LFPs during tremor and tremor-free periods from seven PD subjects. In order for viable

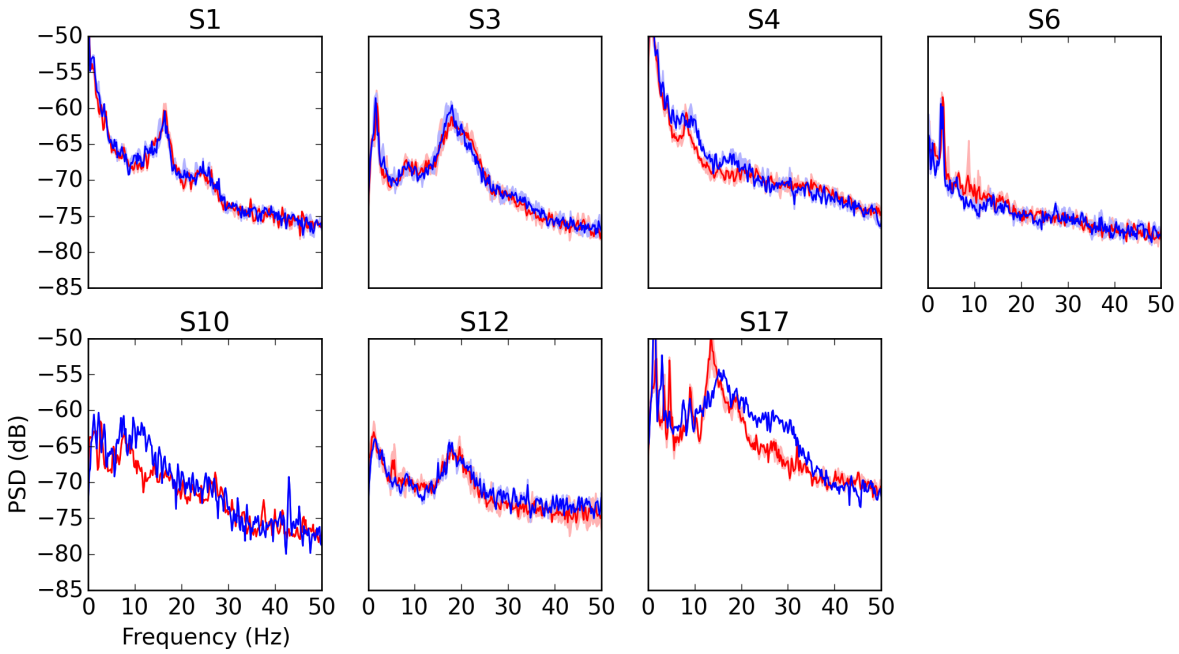

Figure 2.3: "Averaged" LFP spectra during tremor (red) and tremor-free (blue) periods for each subject. Spectra are shown as median and interquartile range.

tremor detection using signals from chronically implanted DBS electrodes, there must be differences in spectral features (e.g. PSD) extracted from these signals during rest and tremor. From each PD subject, between 1 and 6 periods each of tremor and tremor-free recordings were selected to be used for spectral analysis (depending on the total amount of data for a subject, and how clear tremor and tremor-free periods were). Then, from these data, the 30 seconds of data that had the highest and lowest average tremor amplitude were selected as the "best" for tremor and tremor-free periods, respectively. Across the data pooled from all seven subjects, there were significant differences in PSD bands between 4-8 Hz and 8-12 Hz (Wilcoxon signed-rank test, Benjamini-Hochberg correction for multiple comparisons) between tremor and tremor-free LFP activity (Fig. 2.2, left panel). These significant differences, however, are present in the "best" data (i.e. largest tremor vs. most absent from tremor). For tremor detection, these differences in spectral power must be consistent within a given subject over extended amounts of data. This distinction in the quality of spectra in neural activity is important because of the random fluctuations in tremor characteristics inherent in PD (i.e tremor amplitude changes over time).

To examine the consistency of these differences in spectral power, the PSD across all tremor and tremor-free periods selected for spectral analysis for a given subject was averaged to yield a single tremor-free spectrum and a single tremor spectrum for each subject. Using all the tremor/tremor-free data available for the subjects instead of the just the "best" data, the sig-

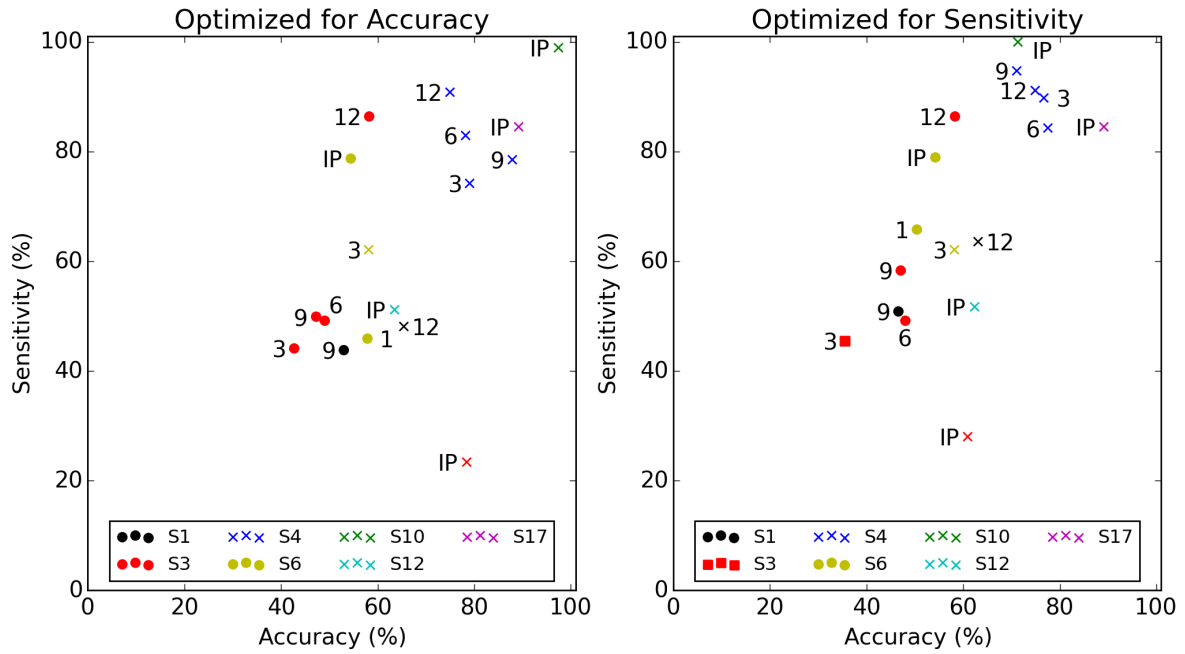

Figure 2.4: Classifier performance for all visits for each of the seven subjects. Classifiers were optimized individually for overall accuracy (**left panel**) and sensitivity (**right panel**). All visits for a given subject are marked in the same color. Data points are labeled with the visit they were calculated from. X markers indicate significantly above-chance performance, circle markers indicate performance no different from chance and square markers indicate significantly below-chance performance (McNemar's test; $p < 0.05$).

nificant differences in the tremor and tremor-free spectra disappeared (Fig. 2.2, right panel). In most of the subjects, there is little difference in the median tremor and tremor-free spectra, both in frequency range and magnitude of the PSD (Fig. 2.3; no within-subject statistics reported because most subjects lacked sufficient data). Additionally, the distributions of the PSD estimates for tremor and tremor-free often completely overlap. The small difference between tremor-free and tremor spectra and the large variance in both spectra suggest that using signals from the STN to detect tremor will be unsuccessful for the majority of subjects. However, a few of the subjects had frequency ranges with some separation between the distributions (S4, 10-20 Hz), providing hope that tremor detection may be successful in these subjects.

Next, the ability to detect tremor using a binary classifier with neural features was examined using data from three of the Parkinson's subjects. STN LFP data were first chunked using a 5-second window, and PSD between 5 and 30 Hz in 1-Hz bins was used for features. Classifier performance was examined for each of a given subject's visits that had sufficient tremor and tremor-free recordings, and classifiers were individually optimized for both accuracy and sensitivity to examine the effect of optimizing for each of the different metrics. For only about half of all the visits, whether optimizing for either accuracy or sensitivity, performance was

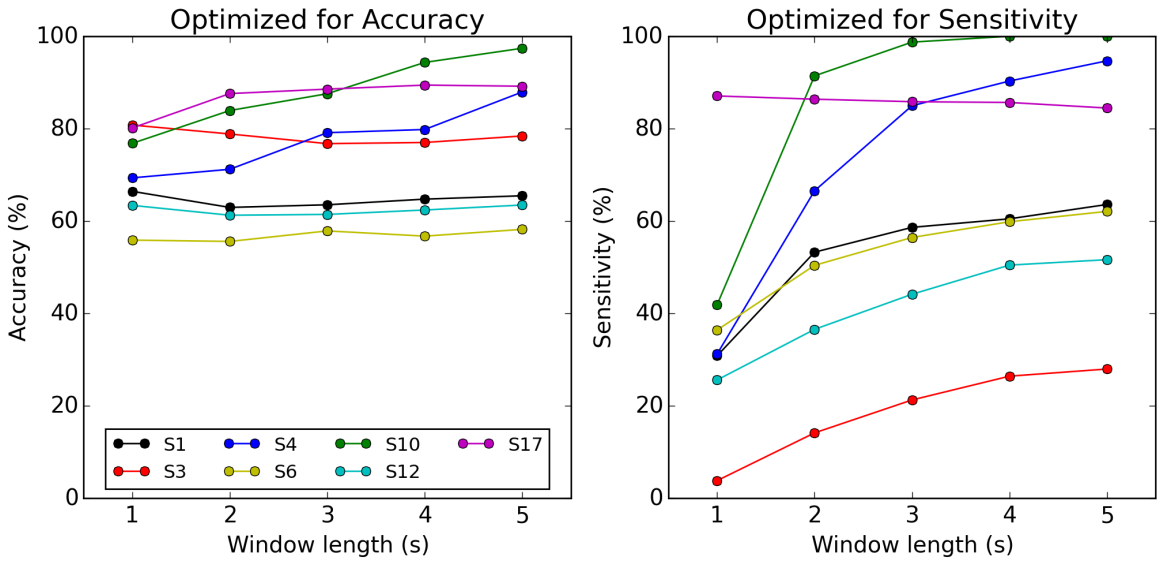

Figure 2.5: Effect of window length on classifier performance for seven subjects. Classifiers were optimized individually for overall accuracy (**left panel**) and sensitivity (**right panel**) with chunking window lengths from one to five seconds, using data from the visit that had the highest classifier performance for the metric being optimized. Data points are labeled with the visit they were calculated from. All visits for a given subject are marked in the same color. All classifiers had performance significantly greater than chance (McNemar's test; $p < 0.05$).

significantly better than chance (McNemar's test; $p < 0.05$) (Fig. 2.4). For one visit from S3, when optimized for sensitivity, performance was actually significantly worse than chance (accuracy = 38.0%; McNemar's test, $p < 0.05$). Only one of the seven subjects, S4, had classifier performance with its given optimized metric consistently greater than 75% for multiple visits (S10 and S12 also had accuracy greater than 75%, but they each only had one visit). In general, optimizing for one or the other metric yielded similar performance, with slight increases in the optimized metric compared to the other.

The classifiers described above were trained and tested using features extracted from a 5-second, sliding window on the STN LFP data. This relatively long window length was used in an attempt to average out some of the variance in PSD estimates in hopes of improving classifier performance. In reality, a 5-second window would be far too long for an actual CLDBS system, as such a long window would introduce a long delay between the onset of tremor and the response of the stimulator. To examine the effect of the chunking length on classifier performance, I repeated the above analysis, varying the amount of data in chunks between 1 and 5 seconds. PSD was still calculated using Welch's method with a 1-second Hann window and 50% overlap, with PSD in 1 Hz bins between 5 and 30 Hz being used as features for the classifier. For all of the subjects, classifier performance generally improved as window length increased, as

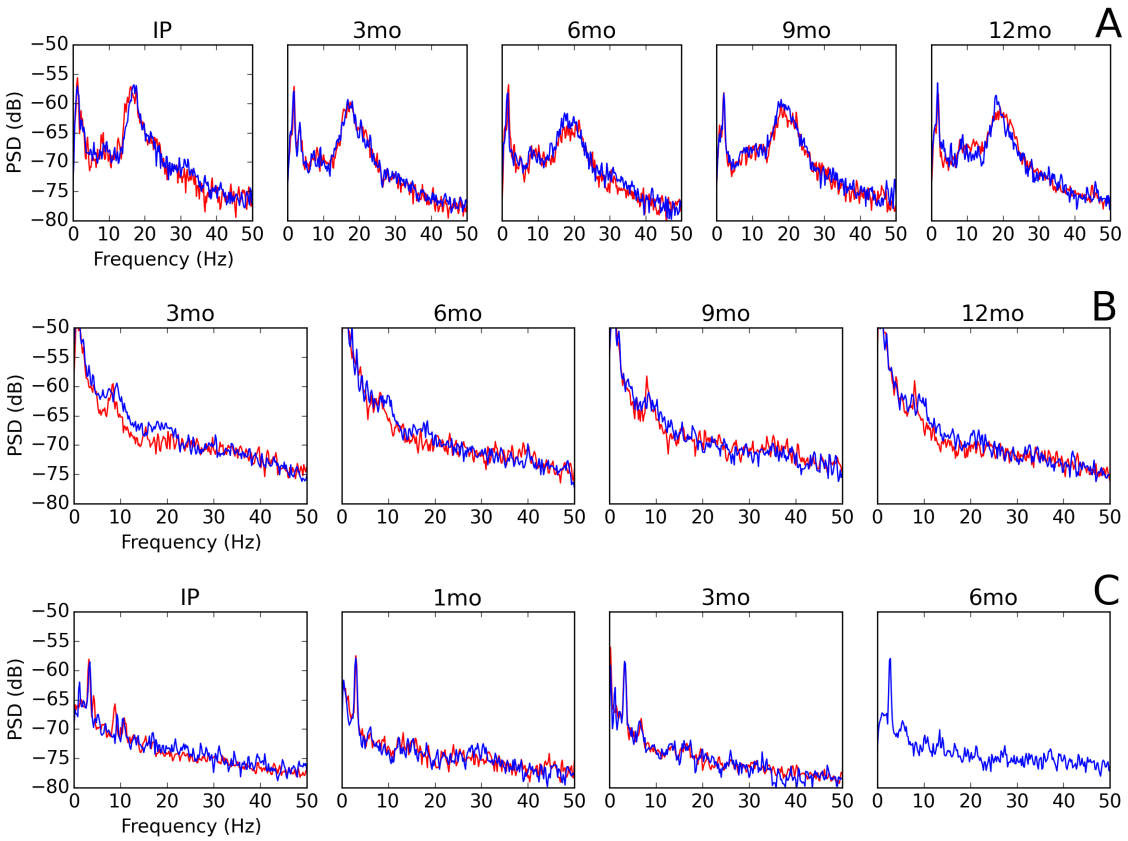

Figure 2.6: Tremor-free (blue) and tremor (red) spectra over the course of several visits for three separate subjects. Spectra are were calculated from all the data selected for spectral analysis (between one and six periods, each with 30-60 seconds of data; in some cases an additional period had to be added to the set for a given subject in order to have data for each time point). Spectra are shown as median and interquartile range (for subjects with only one period selected for analysis, no range is shown). Data in panels A, B and C are from subjects S3, S4 and S6, respectively.

expected (Fig. 2.5). However, there were large discrepancies when optimizing for the different metrics. When optimized for accuracy, the window length only slightly increased the metric. However, when optimizing for sensitivity, window length had a large effect on performance. For all window lengths and for all subjects performance was greater than chance (McNemar's Test, p-value < 0.05; only data from visit showing best classifier performance was used to examine effect of window length).

Next, the ability to detect Parkinsonian tremor from deep-brain neural signals recorded from chronically implanted DBS systems over extended periods of time was examined. Data from three subjects who had between four and five visits each over a period of 6-13 months were used. First, median spectra during rest and tremor for the three subjects were examined for the time frames under consideration. For subject S4, there were consistent differences in average PSD between 10 and 20 Hz over the course of the visits, and the variance of the PSD in this range was actually quite small (Fig. 2.6B). For subjects S3 and S6, although the shape of the

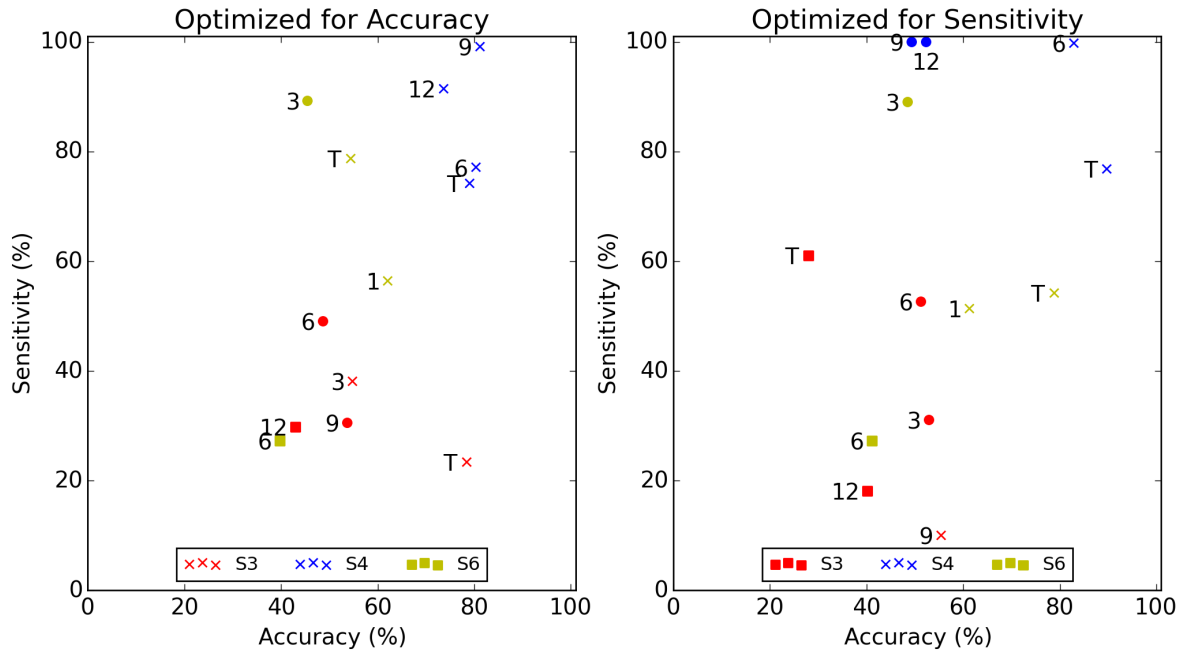

Figure 2.7: Classifier performance over the course of several clinical visits for three separate subjects. Classifiers were trained on data from an initial visit and optimized individually for overall accuracy (**left panel**) and sensitivity (**right panel**), and then tested on data from subsequent visits. All visits for a given subject are marked in the same color with the visit, in months, from which they were calculated ("IP" is initial programming visit). X markers indicate significantly above-chance performance, circle markers indicate performance no different from chance and square markers indicate significantly below-chance performance (McNemar's test; $p < 0.05$). Data points are labeled with the visit they were calculated from ("T" corresponds to the training session, which are shown as 2-fold cross-validation scores).

tremor-free and tremor spectra were quite consistent over the course of several visits, there was little difference between the two states (Fig. 2.6A, 2.6C).

For these three subjects, a classifier was trained on data from the first visit with sufficient data (3 month visit for S4, initial visit for S3 and S6) using two-fold cross-validation and optimizing individually for accuracy and sensitivity. The classifiers were then used to detect tremor for each of the subsequent visits. When optimizing for accuracy, 60% of visits had performance better than chance ($p < 0.05$; McNemar's test), (Figure 2.7) but half of these above-chance visits were from S4, and only that subject's visits consistently had accuracies above 75%. There was a visit each for S3 and S6 that had performance worse than chance ($p < 0.05$; McNemar's test) when optimizing for either metric. When optimizing for sensitivity, only 30% of visits had above chance performance, while 30% had significantly worse performance than chance ($p < 0.05$; McNemar's test). It appears that optimizing for sensitivity resulted in more overfitting than did optimizing for accuracy, shown by the higher sensitivity value for the training visit than for the testing visits for a given subject (training visits denoted by "T").

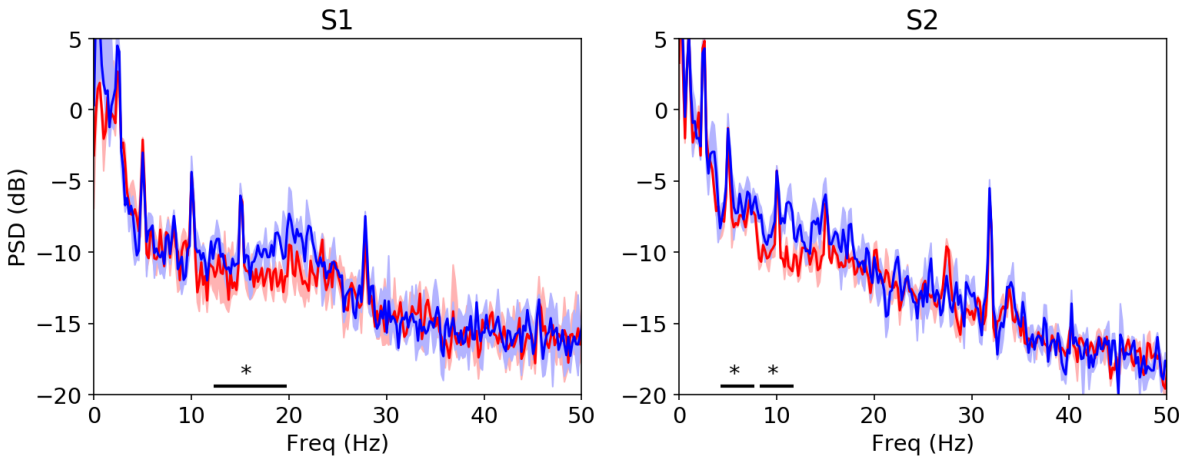

Figure 2.8: LFP spectra during tremor-inducing movement (red) and rest (blue) for each ET subject. Spectra are shown as median and interquartile range. There was a significant difference in low beta (12-20 Hz) band between rest and tremor for subject 1 and significant differences in theta (4-8 Hz) and alpha (8-12 Hz) for subject 2.

2.3.2 Essential Tremor

Next, I sought to answer the question **to what extent can essential tremor can be detected from chronically-implanted DBS electrodes?** As with Parkinson's disease, I first examined spectra during rest and tremor-inducing movement in two subjects during the course of a single visit. Because of the small number of subjects and the ability to reliably and repeatedly induce tremor, single subject statistics were used for these data, rather than the within-subject statistics used for analysis of the Parkinson's data. For this analysis, 4-5 movement epochs and 4-5 rest epochs, each around 30 seconds in duration, were used for PSD estimation. In S1, there was a significant difference in PSD in low beta frequencies (12-20 Hz) between rest and tremor-inducing movement spectra (Fig. 2.8, left panel; Mann-Whitney-U test with Benjamini-Hochberg correction for multiple comparisons, $p < 0.05$). In S2, there were significant differences between rest and tremor-inducing movement spectra in theta (4-8 Hz) and alpha (8-12) bands (Fig. 2.8, right panel; Mann-Whitney-U test with Benjamini-Hochberg correction for multiple comparisons, $p < 0.05$). The significant differences in power during rest and tremor-inducing movement in these subjects suggest that it may be possible to detect essential tremor, or at least the movement that causes tremor, using VIM neural activity as a signal source.

To examine this possibility, I trained a classifier on neural features extracted from the VIM signal recorded during rest and movement for each subject. These features consisted of PSD between 4-30 Hz in 1 Hz bins, calculated using a 1-second sliding window. All the data recorded during the session were split into two halves, and a logistic regression classifier was trained on

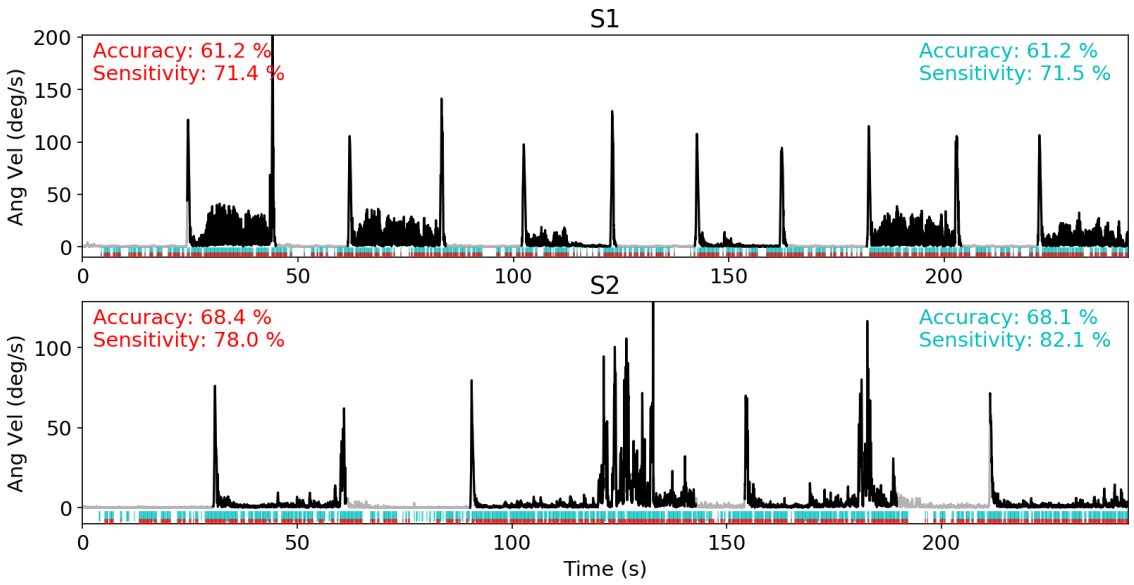

Figure 2.9: Classifier performance for each subject for one session using a one-second sliding window for creating features. Black traces are gyroscopic data and red raster is classifier output. Black dashed line separates training and test data. Cyan raster/text corresponds to classifier optimized for sensitivity, red raster/text corresponds to classifier optimized for sensitivity.

each half and tested on the other half (Fig. 2.9). All metrics reported are the average for the two classifiers. For S1, the classifiers had an accuracy and sensitivity of 61.2% and 71.4%, respectively, when optimized for accuracy and metrics of 61.2% and 71.4% when optimized for sensitivity. For S2, the classifiers had an accuracy and sensitivity of 68.4% and 78.0%, when optimized for accuracy. When optimized for sensitivity, the metrics had values of 68.1% and 82.1%. For both subjects, classifier performance was significantly greater than chance (McNemar's test; $p < 0.01$). As with Parkinson's disease, I examined the effect of window length on classifier performance. The length of each data chunk was varied between 1 and 5 seconds and then its PSD was estimated using Welch's method. The window length did not have a large effect when optimizing for accuracy nor sensitivity (Fig. 2.10).

2.4 Discussion

The purpose of these analyses were to determine the extent to which neural signals recorded from deep brain structures using a chronically implanted DBS system can be used to detect tremor or tremor-inducing movement. To examine this issue, distributions of PSD derived from LFPs during rest and tremor (or tremor-inducing movement) largely overlapped for most of the subjects in both PD and ET. In PD, there were significant differences in several frequency bands when using the most distinguishing rest and tremor spectra. However, this difference

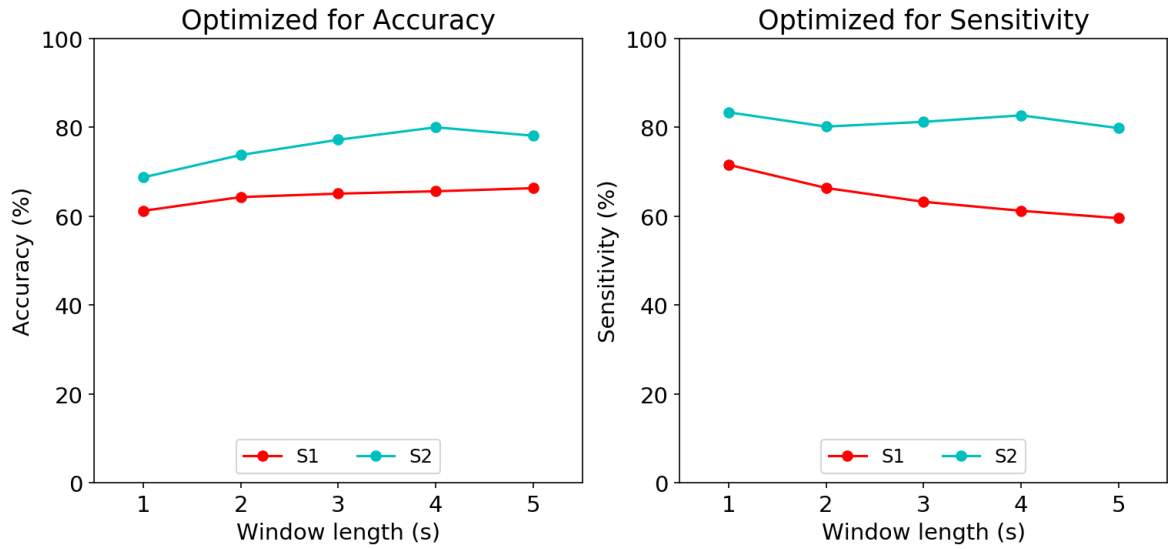

Figure 2.10: Effect of window length on classifier performance for both ET subjects.

disappeared when using all the data available for spectral analysis, instead of just using the best data. It should be noted, that the "average" spectra still didn't even include all the data from each subject, just those periods that were as unambiguous to label as tremor or tremor-free as possible. Therefore, in reality, the tremor and tremor-free spectra would probably be even more indistinguishable. Accordingly, Parkinsonsian tremor detection using these features was largely unsuccessful. Unsurprisingly, the PD subject with the best classifier performance had PSD distributions that showed some separation in spectra during tremor and tremor-free periods. The subjects with the worst performance had little to no separation between tremor and tremor-free spectra. It is interesting to note that classifier performance from different visits was consistently grouped for a given subject. This suggests that there are likely to be subject-specific factors that influence performance, rather than just a categorical problem with signals originating from the STN. Some of these potential subject-specific factors are discussed below.

In the data recorded from ET subjects, both of the subjects had significant differences between tremor-inducing movement and rest in several frequency bands. However, both ET subjects had poor classifier performance when detecting tremor. The actual output of the classifier for both subjects, especially S2, tended to be a positive prediction most of the time. This led to high sensitivities (very few false negatives) for the classifiers, but low accuracies. This likely stems from underfitting of the classifiers during training, which might arise from the high variance in features (i.e. the model is not complex enough to capture variance in data).

In order to begin exploring possible tremor-detection optimization, the window length used

to ”chunk” data was varied from 1-5 seconds. For PD and ET subjects, this had little effect on accuracy, but had a dramatic effect on sensitivity for PD subjects. It is interesting to note that although the ”chunk” length was varied, the Hann window length used during the PSD estimation was not, so in all cases a given chunk would yield the same number of features. However, using longer window lengths, especially with tremor that is not rapidly changing (i.e. spontaneously coming and going), would act to decrease the variance of the PSD estimates (features). Higher variances in the features at lower window lengths might cause underfitting of the logistic regression model, causing it to output relatively more negative predictions. This wouldn't affect accuracy as much, since tremor was present around half of the time for most visits, but it would have a large effect on sensitivity. Indeed, in several of the patients, the ratio of positive predictions increases dramatically with window length, confirming this hypothesis.

Next, to mimic the situation where a symptom-detection model is trained during an initial clinical visit and then used to control stimulation over extended periods of time, a classifier was trained on data from one visit and then used to detect Parkinsonian tremor in subsequent visits without retraining. One of the three PD subjects that had multiple visits showed consistent differences in PSD estimates during rest and tremor between 10-20 Hz and accordingly, had good tremor detection up to 9 months after training. The other two subjects, on the other hand, showed little separation in PSD distributions between tremor and tremor-free periods and correspondingly had poor tremor detection up to 12 months after training. The shape of the spectra were remarkably consistent for all three subjects over the time courses observed; however, separation between tremor and tremor-free spectra was simply not present for two of three, leading to poor performance of the classifier.

These results suggest that for most subjects, it appears that **neither Parkinsonian tremor nor essential tremor can be reliably detected from deep brain electrodes over any period of time**. This failure appears to stem from the large variations in PSD estimates during tremor and tremor-free periods that occur for the majority of the subjects and the lack of correlation between neural activity recorded from deep brain structures and tremor (or tremor-inducing movement). This high variability and lack of correlation could stem from several different causes, ranging from surgical or implant issues to physiological reasons.

One of the most likely reasons for the lack of difference in LFP oscillatory content between tremor and tremor-free periods is the placement of the DBS electrode. The nucleus targeted by DBS in all the PD subjects was the STN, which is one of the most common targets for

treatment of PD. It is known that the STN is functionally organized [9], and that the region of the STN involved in movement (and tremor) is somatotopically organized [14]. Because of the size, location and somatotopy of the STN, it is not surprising that there are often slight errors in DBS electrode placement, where the electrode may not penetrate the optimal location [13]. These small errors in placement may not compromise therapy, since stimulation voltage can be increased enough to enlarge the stimulated region to encompass the targeted area. However, even a small error may compromise the ability to sense LFPs reflecting activity in the tremoring limb, due to the small size of the targeted area and local nature of the LFP. Similar arguments can be made for the VIM of the thalamus, which was the target for the ET subjects. Another factor that complicates the ability to sense LFPs from the somatotopically correct area is the fact that electrode contacts used for stimulating cannot also be used for simultaneous recording. Since stimulation is often given in a bipolar configuration using the most effective contact pair (and was done so for all the subjects in this study), it is likely that using different contacts for recording would yield sub-optimal results.

Furthermore, after implantation, DBS leads are not necessarily completely immobile, and can shift location slightly [5]. Any movement of the leads could compromise the ability to sense the localized LFP, based on the arguments outlined in the above paragraph. A potential solution to this problem involves sensing LFPs from all electrode contacts on the lead; currently, the capabilities of the DBS device used limit to only two contacts being used in a differential configuration, providing a single channel of data. Future technology will allow for recording from multiple contact pairs while also increasing the number and density of contacts. This increased ability to sense more signals from smaller areas will increase the likelihood of sensing from the somatotopically correct area, as long as the DBS lead impinges correctly on the target region of interest. Somewhat related to suboptimal lead placement and lead movement is the foreign body response to the DBS lead. Encapsulation of the lead can occur [6][8][15], increasing the impedance of the electrodes and decreasing the ability to sense small-amplitude LFPs.

While the above issues are caused by the DBS implant surgery and the device itself, there could also be physiological reasons that make detection of tremor from deep brain structures difficult. PD and ET are complex neurodegenerative diseases that can manifest differently in different subjects. Not only can the symptoms present in one subject be different from those in another, but the affected body regions can be different. In subjects that have tremor, the characteristics of the tremor, such as frequency and amplitude can be different. All of

this complexity in the outward manifestations of these movement disorders is mirrored and even amplified when examining the neural signals underlying them. How neural signatures of different symptoms, such as tremor and bradykinesia, interact and obscure each other is not well understood, and can make detection of any of the symptoms difficult, especially in PD. Furthermore, tremor can be continuously present, albeit with a very small amplitude that is not necessarily outwardly noticeable, especially in PD. The presence of this small-amplitude tremor can corrupt a classifier's ability to distinguish between actual tremor and tremor-free periods.

A last potential reason for the difficulty in detecting tremor from deep nuclei stems from the algorithms used for detection. The logistic regression classifier is a relatively simple linear method for separating features belonging to two different classes. It is possible that using more complicated nonlinear or multi-class classifiers would improve performance. This, however, seems unlikely, given the small amount of separation of the PSD features used for the classifiers. A more likely classifier-related cause for detection problems is the small amount of training data available to the classifiers. Classifiers were trained only using several minutes of data. It is likely that more training data will improve classifier performance, although the improvement may not be dramatic. It is expected that more training data would decrease the variance of the features, but this decrease in variance might not be enough to improve performance since the separation between the LFP features of the two classes is so small and inconsistent. It is interesting to note that one of the highest performing classifiers (S4, visit at 9 months) was actually trained using less data than the majority of the other sessions for the other subjects. This suggests that while increasing the amount of data may improve classifier performance, it cannot overcome other factors that lower the quality of the data.

At least one study has examined STN LFPs during tremor and rest and found that several frequency bands showed significant differences [11]. However, the results presented in this chapter don't necessarily contradict the results from that study. First, there were significant differences in tremor and rest spectra for both studies at the group level. However, the study by Qasim, et al, only used tens of seconds or less for spectral estimation, and these signals were recorded intraoperatively during DBS placement surgery. Collecting data in this manner prohibits the examination of these significant spectral differences over longer periods of time, and also mitigates some of the potential confounding factors described above, especially those related to constraints on signal acquisition using implanted hardware.

2.5 Chapter Summary

In this chapter, I presented data collected from several subjects who had been implanted with DBS hardware for the treatment of PD or ET. Using signals recorded from the DBS electrode (STN for PD, VIM for ET), I found that there were some differences in the oscillatory content of neural activity during rest and tremor (or tremor-inducing movement). However, these differences in neural activity were inconsistent, and consequently, symptom detection using these signals was largely unfruitful.

References

[1] E. Bakstein, J. Burgess, K. Warwick, V. Ruiz, T. Aziz, and J. Stein, "Parkinsonian tremor identification with multiple local field potential feature classification.," *Journal of neuroscience methods*, vol. 209, no. 2, pp. 320–30, Aug. 2012.

[2] E. Bakstein, K. Warwick, J. Burgess, O. Stavdahl, and T. Aziz, "Features for detection of Parkinson's disease tremor from local field potentials of the subthalamic nucleus," *2010 IEEE 9th International Conference on Cyberntic Intelligent Systems*, pp. 1–6, Sep. 2010.

[3] D. Basha, J. O. Dostrovsky, A. L. Lopez Rios, M. Hodaie, A. M. Lozano, and W. D. Hutchison, "Beta oscillatory neurons in the motor thalamus of movement disorder and pain patients.," *Experimental neurology*, vol. 261, pp. 782–790, Sep. 2014.

[4] Z. Blumenfeld and H. Brontë-Stewart, "High Frequency Deep Brain Stimulation and Neural Rhythms in Parkinsons Disease," *Neuropsychology Review*, vol. 25, no. 4, pp. 384–397, 2015.

[5] J. M. Bronstein, M. Tagliati, R. L. Alterman, A. M. Lozano, J. Volkmann, A. Stefani, F. B. Horak, M. S. Okun, K. D. Foote, P. Krack, R. Pahwa, J. M. Henderson, M. I. Hariz, R. A. Bakay, A. Rezai, W. J. Marks, E. Moro, J. L. Vitek, F. M. Weaver, R. E. Gross, and M. R. DeLong, "Deep Brain Stimulation for Parkinson Disease," *Archives of Neurology*, vol. 68, no. 2, p. 165, 2011.

[6] C. R. Butson, C. B. Maks, and C. C. McIntyre, "Sources and effects of electrode impedance during deep brain stimulation," *Clinical Neurophysiology*, vol. 117, no. 2, pp. 447–454, 2006.

[7] C. Camara, P. Isasi, K. Warwick, V. Ruiz, T. Aziz, J. Stein, and E. Bakštein, "Resting tremor classification and detection in Parkinson's disease patients," *Biomedical Signal Processing and Control*, vol. 16, pp. 88–97, Feb. 2015.

[8] C. Haberler, P. R. Mazal, P. Pilz, K. Jellinger, M. M. Pinter, J. A. Hainfellner, and H. Budka, "No Tissue Damage by Chronic Deep Brain Stimulation in Parkinson's Disease," *Ann Neurol*, vol. 48, no. 3, pp. 372–398, 2000.

[9] C. Lambert, L. Zrinzo, Z. Nagy, A. Lutti, M. Hariz, T. Foltynie, B. Draganski, J. Ashburner, and R. Frackowiak, "Confirmation of functional zones within the human subthalamic nucleus: Patterns of connectivity and sub-parcellation using diffusion weighted imaging," *NeuroImage*, vol. 60, no. 1, pp. 83–94, 2012.

[10] S. Pan, S. Iplikci, K. Warwick, and T. Z. Aziz, "Parkinson's Disease tremor classification – A comparison between Support Vector Machines and neural networks," *Expert Systems with Applications*, vol. 39, no. 12, pp. 10 764–10 771, Sep. 2012.

[11] S. E. Qasim, C. de Hemptinne, N. C. Swann, S. Miocinovic, J. L. Ostrem, and P. A. Starr, "Electrocorticography reveals beta desynchronization in the basal ganglia-cortical loop during rest tremor in Parkinson's disease," *Neurobiology of Disease*, vol. 86, pp. 177–186, 2015.

[12] C. Reck, E. Florin, L. Wojtecki, H. Krause, S. Groiss, J. Voges, M. Maarouf, V. Sturm, A. Schnitzler, and L. Timmermann, "Characterisation of tremor-associated local field potentials in the subthalamic nucleus in Parkinson's disease.," *The European journal of neuroscience*, vol. 29, no. 3, pp. 599–612, Mar. 2009.

[13] J. D. Rolston, D. J. Englot, P. A. Starr, and P. S. Larson, "An unexpectedly high rate of revisions and removals in deep brain stimulation surgery: Analysis of multiple databases," *Parkinsonism & Related Disorders*, pp. 10–15, 2016.

[14] P. Romanelli, G. Heit, B. C. Hill, A. Kraus, T. Hastie, and H. M. Brontë-Stewart, "Microelectrode recording revealing a somatotopic body map in the subthalamic nucleus in humans with Parkinson disease.," *Journal of neurosurgery*, vol. 100, pp. 611–618, 2004.

[15] D. a. Sun, H. Yu, J. Spooner, A. D. Tatsas, T. Davis, T. W. Abel, C. Kao, and P. E. Konrad, "Postmortem analysis following 71 months of deep brain stimulation of the subthalamic nucleus for Parkinson disease.," *Journal of neurosurgery*, vol. 109, no. 2, pp. 325–329, 2008.

[16] P. Tass, D. Smirnov, A. Karavaev, U. Barnikol, T. Barnikol, I. Adamchic, C. Hauptmann, N. Pawelcyzk, M. Maarouf, V. Sturm, H.-J. Freund, and B. Bezruchko, "The causal relationship between subcortical local field potential oscillations and Parkinsonian resting tremor," *Journal of Neural Engineering*, vol. 7, no. 1, p. 016 009, 2010.

[17] S. Wang, Y. Chen, M. Ding, J. Feng, J. Stein, T. Aziz, and X. Liu, "Revealing the dynamic causal interdependence between neural and muscular signals in Parkinsonian tremor," *Journal of the Franklin Institute*, vol. 344, no. 3-4, pp. 180–195, May 2007.

[18] D. Wu, K. Warwick, Z. Ma, M. N. Gasson, J. G. Burgess, S. Pan, and T. Z. Aziz, "Prediction of Parkinson's disease tremor onset using a radial basis function neural network based on particle swarm optimization.," *International journal of neural systems*, vol. 20, no. 2, pp. 109–16, Apr. 2010.

Chapter 3

Offline Tremor Detection From Cortical Electrodes

3.1 Introduction

This chapter presents work done to address Aim 2 of this dissertation, to what extent can essential tremor be reliably detected **from neural signals recorded from cortical areas** using a chronically-implanted DBS system? As opposed to the results discussed in chapter 2, this chapter will focus solely on ET subjects, rather than both ET subjects and PD subjects.

As discussed in chapter 2, closed-loop deep brain stimulation (CLDBS) could potentially be implemented using several different neural signals. The benefits to using neural signals, compared to movement signals, are discussed in the introduction to that chapter. Experiments using neural signals, specifically those recorded from DBS electrodes, to detect tremor were also presented and discussed. Those results showed that tremor detection using DBS electrodes was difficult and largely unsuccessful, and several potential reasons for this poor performance were postulated. The factor that seems most likely to cause difficulty in detecting tremor from deep brain regions is the placement of the DBS electrode relative to the area of interest. Because of the small brain areas being targeted and the coarse spatial resolution of the DBS electrode, it is no surprise that successfully sensing the correct signal is difficult.

Sensing from other brain areas, such as motor cortex, may circumvent these challenges. There is a rich literature characterizing network activity from many cortical areas during both normal and pathological movement in a variety of animal models and human subjects. This work has been done using a variety of sensing modalities, each with its own benefits and draw-

backs, such as penetrating microelectrodes, electrocorticography (ECoG), electroencephalography (EEG), magnetoencephalography (MEG) and functional magnetic resonance imaging (fMRI). The majority of these recording modalities sense aggregate activity from large groups of neurons. One of the most conspicuous changes in cortical activity (LFPs for EEG/ECoG) is beta-band (12-30 Hz) desynchronization (decrease in oscillatory power), visible using most, if not all, of the sensing modalities above. Beta-band desynchronization is a spatially widespread phenomenon, occurring over large areas of motor and somatosensory cortex during movement [8]. Cortical beta-band desynchronization also typically involves large changes in power in an already large amplitude signal, making it a relatively easy event to detect, especially compared to the very small-amplitude signals recorded from deep brain nuclei [6]. These factors suggest that signals recorded from motor cortex are likely to be useful for detecting tremor-inducing movement in ET.

A further benefit to using cortical signals instead of deep brain signals for detecting tremor is the integrity of the signal during stimulation. In order for a CLDBS system to work successfully, tremor detection must be possible while stimulation is off to detect the onset of movement, but also while stimulation is on, to detect the cessation of movement. During stimulation, the stimulus artifact seen in the cortex is much smaller in amplitude than in the deep brain region being stimulated, making symptom detection during stimulation more feasible from cortical areas.

If using cortical signals, there are several recording modalities available, as mentioned above. The recording modality that is most amenable to CLDBS is ECoG, for several reasons. First and foremost, its proximity to the cortical surface means it can provide high-quality, high-bandwidth signals with much higher spatial resolution than other, non-invasive modalities, like EEG and MEG. Second, ECoG recording uses hardware that is small enough to be implanted, meaning that no other external devices, such as complex recording caps (EEG) or large, expensive, magnets (MEG,fMRI) would be necessary. Third, ECoG strips can safely be implanted permanently and can sense neural activity over extended periods of time using the same burr hole created for implantation of the DBS electrode [3][4]. Several intra-operative studies have examined cortical activity in ET patients, using ECoG. During DBS implantation surgery, it has been shown using temporarily implanted ECoG electrodes that beta-band desychronization occurs during movement [2][5][11], as it does in persons free from ET.

However, none of the studies mentioned above implanted permanent ECoG electrodes, and

none used cortical data in an attempt to detect tremor-inducing movement in ET; the studies were simply characterizing changes in neural activity as they relate to movement and/or symptoms. To determine if cortical activity from permanently-implanted ECoG electrodes can be used as a signal source for detecting tremor-inducing movement in ET subjects, we used an investigational DBS device that can sense cortical activity from a 4-contact ECoG strip electrode. This electrode was implanted over hand/arm area of primary motor cortex in two subjects with ET, along with their clinical DBS system [4]. With this device, cortical data were recorded during tremor-inducing movement, under both stimulation-off and stimulation-on states. As in chapter 2, classifiers were trained to detect tremor-inducing movements during a prompted movement task using this cortical data. Again, machine learning was used a way to build patient-specific models relating neural activity and tremor-inducing movement that capture nuances in neural signals for each subject [9]. For both subjects, tremor detection using these classifiers was very robust, and unsurprisingly, was much better than when using deep brain signals.

3.2 Methods

3.2.1 Data Collection

All experiments were approved by the FDA (IDE received) and the University of Washington IRB committee, and the patients gave informed consent. The data for this study were collected from two subjects who had been diagnosed with essential tremor (same ET subjects from chapter 2; see Table 3.1 for subject information). Both subjects had been implanted with the Medtronic Activa PC+S® DBS system, with the DBS electrode implanted in the VIM (unilateral) of thalamus. Additionally, both subjects had a four-contact electrocorticography electrode implanted over the central sulcus, approximately covering the hand/arm region of primary motor and primary somatosensory cortex. The placement of the electrocorticography electrodes was verified by coregistered MRI and CT scans, along with the presence of beta-band desynchronization during right-arm/hand movements. Around one month after implantation, each subjects' DBS system was programmed for optimal therapeutic effect. Thereafter, subjects returned for follow-up visits approximately every 6-8 weeks for experiments. We used the ability of the Activa PC+S® system to record LFPs to obtain neural data from the electrocorticography electrode during these experimental visits. The system is capable of streaming a

Table 3.1: Subject Information

Subject	**Sex**	**Age**	**Affected Limb**	**Implant Side**	**Recording Contacts**	**Stimulation Contacts**	**DBS Settings**
S1	M	58	RH	L	8-10	2+/0-	2.5V,140Hz,90µs
S2	M	81	RH	L	9-11	1+/0-	3.7V,130Hz,90µs

single channel of LFP data from the ECoG electrode in a differential configuration. The ECoG contact pairs that yielded the highest-amplitude signal were used for sensing neural activity, and can be seen in Table 3.1.

For ET subjects, during each visit, neural data were recorded while the subject engaged in prompted movement tasks. Specific movements were different for the two subjects because different movements evoked tremor. However, both subjects performed prompted movements using their right arm and hand while in a sitting position (subject S1 brought his hand to his face and held it at his chin, subject S2 mimicked holding and repeatedly twisting a screwdriver). Two different prompt paradigms were used; the first consisted of movements lasting approximately 30 seconds, interspersed with rest periods of a similar duration (termed "LONG" periods). The second consisted of movement lengths taken from a uniform distribution between 3 and 12 seconds, with rest lengths taken from the same distribution (termed "SHORT" periods). For both movement paradigms, 4 minutes of total data were recorded during the task. Both movement paradigms were performed with stimulation OFF and stimulation ON, using the subject's therapeutic parameters (for a total of 4 trials per subject) (see Table 3.1 for stimulation parameters for each subject). Movement activity was recorded using the onboard IMU of a consumer smartwatch, worn on the subject's right wrist. Accelerometer, gyroscope and magnetometer data were sampled at 100 Hz.

During the prompted movement task, LFPs were streamed in real time from the ECoG lead onto a laptop computer. Neural signals were were high-pass filtered at 0.5 Hz and low-pass filtered at 100 Hz. All LFP data were sampled at 422 Hz (10-bit resolution) with a gain of 2000. Subject S1 was in an OFF-medication state during the task, but subject S2 was taking propranolol (beta-blocker) and primidone (anti-convulsant) for treatment of ET.

3.2.2 Data Processing

To determine when the subjects were moving, inertial data from the affected limb was visually inspected to determine periods containing prompted movement and periods free from movement.

To examine differences in cortical activity during movement and rest, PSD was estimated for each movement and rest period during the "LONG" movement paradigm using Welch's method with a Hann window length of 5 seconds with 50% overlap. Log power was averaged over the following five frequency ranges to detect differences between spectra: alpha (4-8 Hz), theta (8-12 Hz), low beta (12-20 Hz), high beta (20-30 Hz) and low gamma (30-50 Hz). Because of the small number of ET subjects, only differences between spectra within individual subjects were examined. Statistical differences within subjects were tested using the Mann-Whitney-U test if a k-test detected a non-normal distribution, otherwise an unpaired t-test was used. Benjamini-hochberg corrections were used for multiple comparisons.

3.2.3 Classifier Training/Testing

Neural features for the training/testing of a classifier for tremor detection were extracted from each trial's cortical recordings by chunking the LFP data into overlapping windows every 200 ms (window length was varied between 1-2 seconds). Each of these chunks had its power spectral density (PSD) estimated using Welch's method with a 1-second Hann window and 50% overlap. Differences in PSD between tremor and tremor-free epochs were largely contained between 4-30 Hz, so PSD in approximately 1 Hz bins in this range was then used as features for the training and testing of a binary classifier. Each of the LFP chunks was labeled as tremor or tremor-free using the visually inspected movement data for ET subjects.

Next, for each of the four different trials (LONG OFF, LONG ON, SHORT OFF, SHORT ON), LFP features and their corresponding labels were divided equally into two sets. Each of the two data sets for a subject was used to train a logistic regression classifier. To prevent overfitting, L_2-norm regularization was used, and the optimal regularization hyperparameter was selected using 2-fold cross-validation. The classifier was optimized for either accuracy or sensitivity (true positive rate, recall) to examine the effect of optimizing for different metrics. All metrics are therefore "cross-validation" scores, rather than "testing" scores, and are reported as the average for the two classifiers. Each feature (PSD in 1 Hz bins between 4 and 30 Hz) from the training set was normalized to have zero mean and unit variance and then used to train a regularized logistic regression classifier. The testing set was normalized by the mean

and variance of the training set, and then the label for each chunk was predicted using the trained classifier. Performance of the classifier was measured with accuracy and sensitivity using the instantaneous tremor amplitude data for ground truth. Above-chance performance was determined using McNemar's test. Accuracies for all classifiers were significantly greater than chance ($p < 0.01$).

For long-term movement detection, cortical data from several different visits for each subject over a course of five to eight months were used. Cortical and movement data were recorded as described above during a prompted movement task (For S1, channel gain was 1000 for the first two visits and 2000 for the last three. Therefore, the raw data for the first two visits were multiplied by a factor of two so that PSD would be similar for all visits). Movement and rest period durations, as well as the total duration of the task, varied from visit to visit. PSD features were extracted from the cortical signals as described above, using Welch's method with a 1-second Hann window and 50% overlap. Classifiers were trained with features from the first visit using 2-fold cross-validation to select hyperparameters for optimizing either accuracy or sensitivity. Classifiers were then used to detect movement in subsequent visits.

3.3 Results

For Aim 2, I sought to answer the question: **can tremor-inducing movement be reliably detected from neural signals recorded from cortical areas using a chronically-implanted DBS system, and if so, is this detection better than detection using signals from deep-brain structures?** To answer this question, I first looked at spectra during a prompted movement task that was designed to induce tremor in two ET subjects. For each subject, spectra were calculated from 4-5 movement and rest periods, and differences in log PSD in five different bands were examined (alpha (4-8 Hz), theta (8-12 Hz), low beta (12-20 Hz), high beta (20-30 Hz) and low gamma (30-50 Hz)).

For both subjects, there were large decreases in power during movement of up to 15 dB across a wide range of frequencies (Figure 3.1A). For each to the two subjects, there were significant differences in all five bands ($p < 0.05$; Mann-Whitney-U test, Benjamini-Hochberg correction for multiple comparisons). These large, consistent differences in PSD between movement and rest suggest that tremor detection using cortical signals will be feasible.

In order to test if cortical signals can be used to detect tremor, a binary classifier was

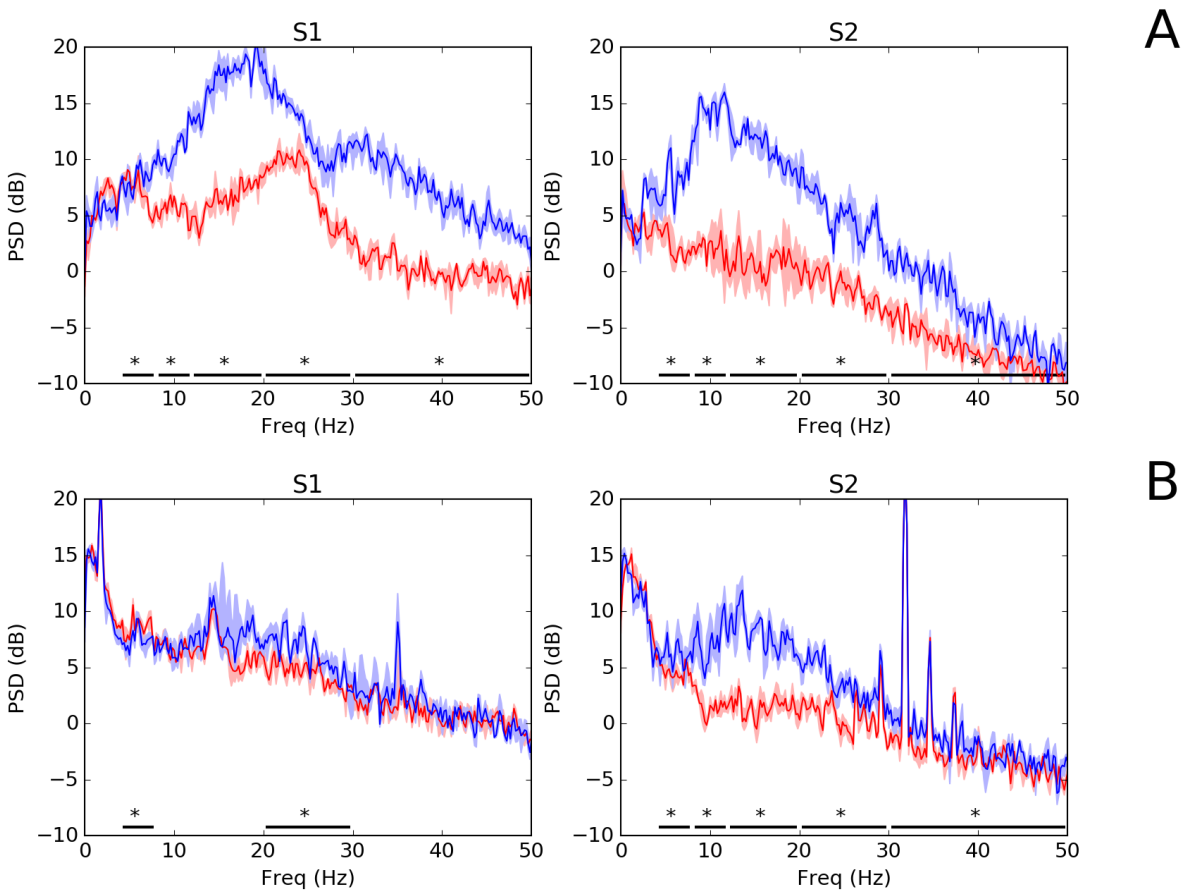

Figure 3.1: Spectra extracted from cortical signals during rest (blue) and movement (red) periods in a prompted movement task. Spectra are shown as median and interquartile range (n=4-5 movement and rest periods per subject, per condition). Significant differences in power in different frequency ranges are shown with a star ($p < 0.05$; Mann-Whitney-U test; corrected for multiple comparisons). Panel A shows spectra with stimulation off, panel B shows spectra with stimulation on.

trained using neural features extracted from the cortical signals. Features were first extracted by estimating PSD with a periodogram using 1-second chunks of data. Two-fold cross-validation was used on the "LONG" period prompted movement data with stimulation OFF to optimize classifiers individually and examine performance. Qualitatively, the classifiers consistently were able to distinguish between movement and rest for both subjects (Figure 3.2A). For S1, accuracy and sensitivity were 75.7% and 92.9%, respectively, when optimized for accuracy, and 75.5% and 93.4%, respectively, when optimized for sensitivity (Table 3.2). For S2, accuracy and sensitivity were 90.6% and 92.5%, respectively, when optimized for accuracy, and 89.1% and 95.9%, respectively, when optimized for sensitivity (Table 3.2).

For effective closed-loop control, tremor detection also needs to be feasible with therapeutic stimulation enabled. To see if movement can still be differentiated from rest with stimulation on, the subjects engaged in the same prompted movement task as described previously, but

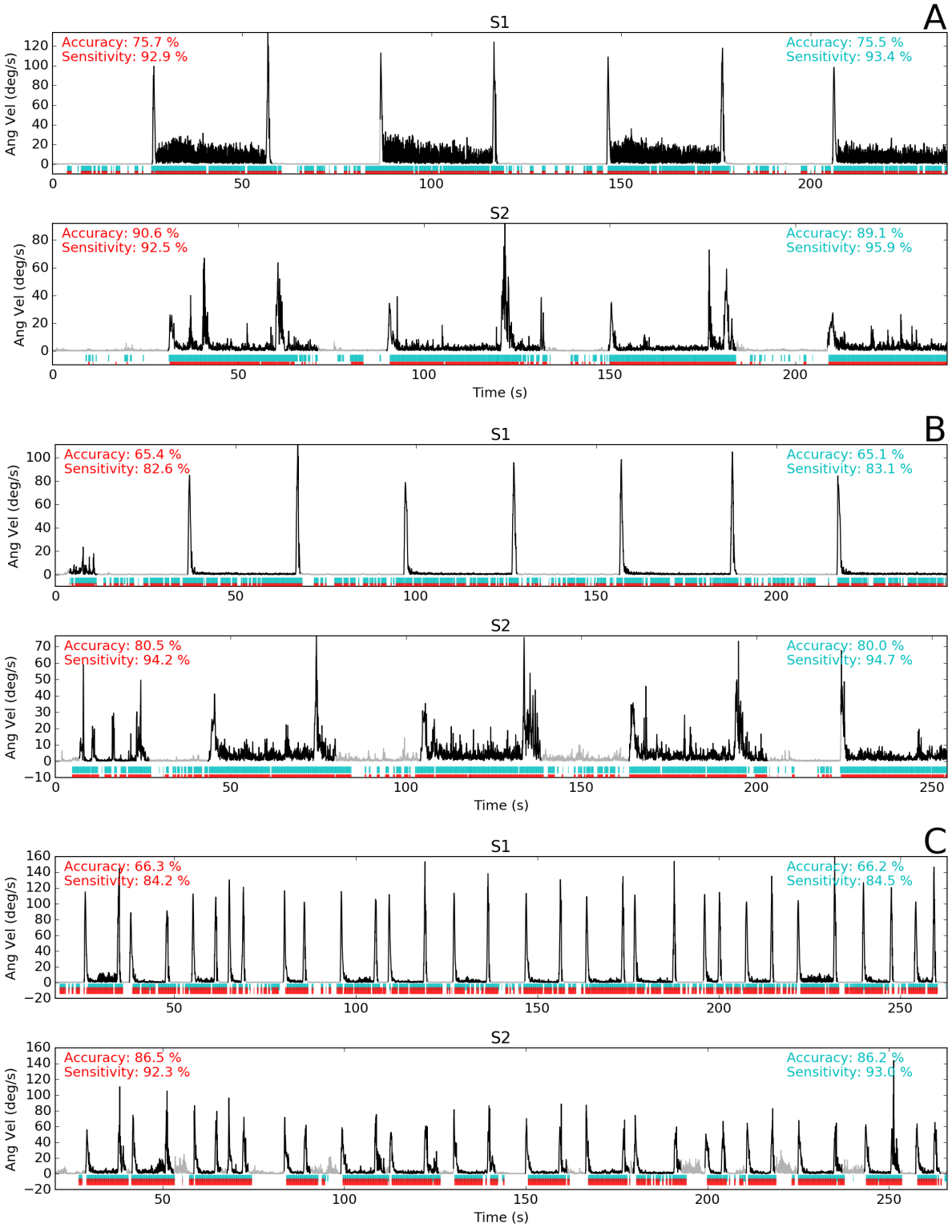

Figure 3.2: Time course of movement detection during different prompted movement tasks under both stimulation off and on conditions. Black/gray trace is gyroscopic data recorded from right arm (black during movement, gray during rest), red/cyan raster traces shown when classifiers detected movement (red is classifier optimized for accuracy, cyan is classifier optimized for sensitivity). Panel A is "LONG" movement task with no stimulation, panel B is "LONG" movement task during stimulation and panel C is "SHORT" movement task with no stimulation.

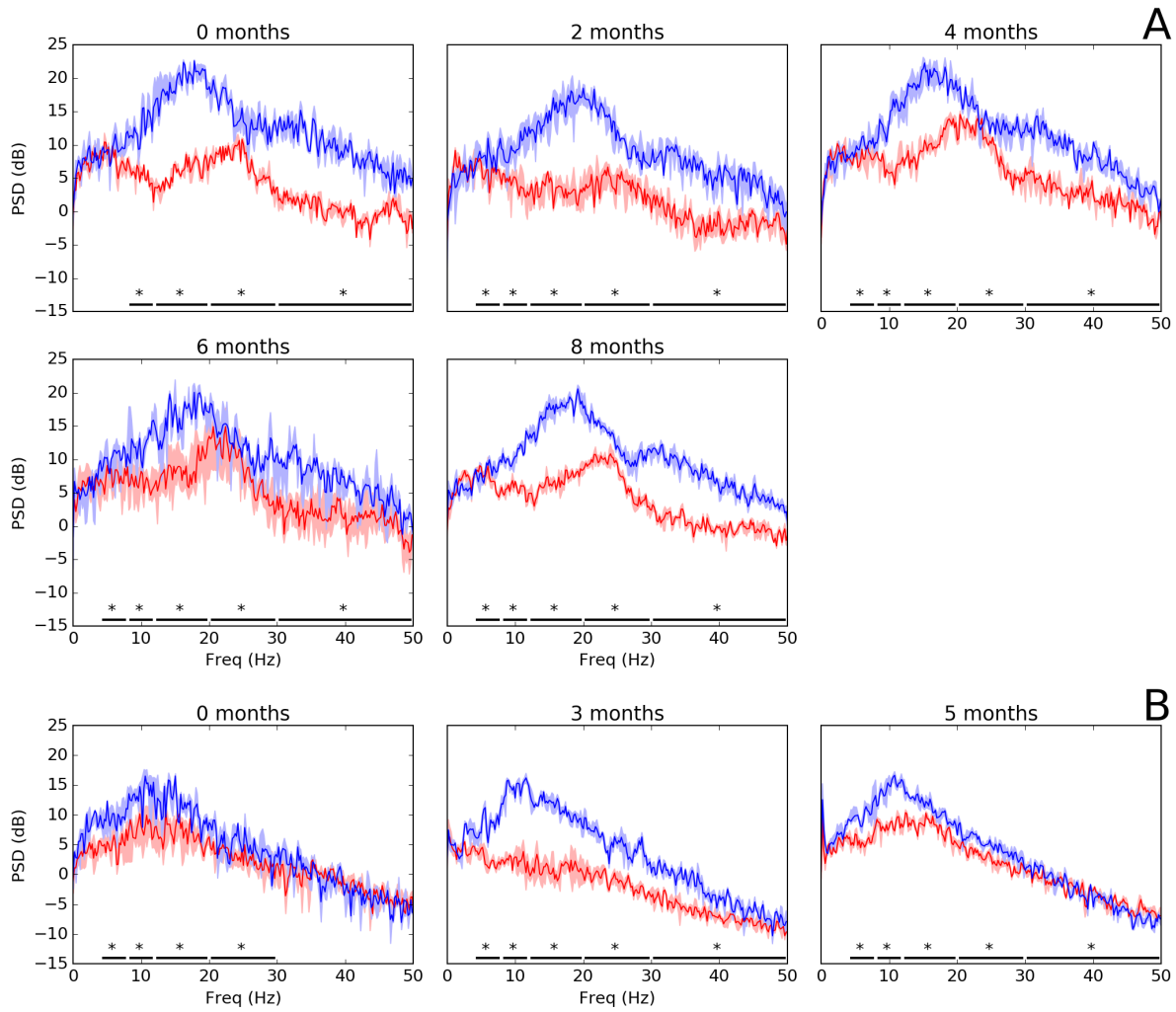

Figure 3.3: Rest (blue) and movement (red) spectra from prompted movement tasks are consistent over the course of several months for both subject S1 (A) and subject S2 (B). Spectra are shown as median and interquartile range (n=4-5 movement and rest periods per subject, per condition, except for spectra at 6 months for subject S1, which contained 16 rest and movement periods that were between 3-12 seconds in duration, resulting in noisier spectra). Significant differences in power in different frequency ranges are shown with a star ($p < 0.05$; Mann-Whitney-U test; corrected for multiple comparisons).

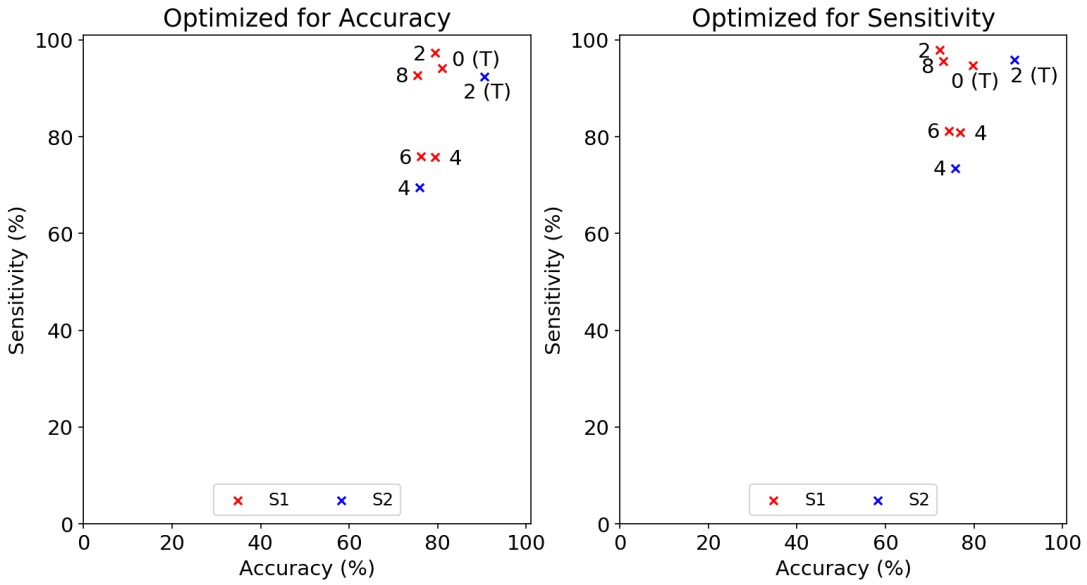

Figure 3.4: Classifier performance when training on an initial visit and detecting movement over the course of several clinical visits. Classifiers were optimized individually for overall accuracy (left panel) and sensitivity (right panel). All visits for a given subject are marked in the same color. X markers indicate significantly above-chance performance, circle markers indicate performance no different from chance and square markers indicate significantly below-chance performance (McNemar's test; $p < 0.05$). Data points are labeled with the visit they were calculated from ("T" corresponds to the training session, which are shown as 2-fold cross-validation scores).

with stimulation enabled. Again, spectra were calculated from each movement and rest period, and differences in the five bands were examined. For both subjects, power across the spectrum was reduced during stimulation by up to 10 dB, especially when at rest (Figure 3.1B). For S1 and S2, during rest, there was a significant decrease in log power in all five bands compared to stimulation off ($p < 0.05$; Mann-Whitney-U test, Benjamini-Hochberg correction for multiple comparisons). For S1 during movement, there was a significant decrease in theta (4-8 Hz), alpha (8-12 Hz), high beta (20-30 Hz), and low gamma (30-50 Hz) bands ($p < 0.05$; Mann-Whitney-U test, Benjamini-Hochberg correction for multiple comparisons). For S2 during movement, there was a significant decrease in theta (4-8 Hz), high beta (20-30 Hz) low gamma (30-50 Hz) bands ($p < 0.05$; Mann-Whitney-U test, Benjamini-Hochberg correction for multiple comparisons).

Despite the effects of stimulation, however, for both subjects, there was still a decrease in power during movement when stimulation was on. For S1, there were only significant differences in theta (4-8 Hz) and high beta (20-30 Hz) bands ($p < 0.05$; Mann-Whitney-U test, Benjamini-Hochberg correction for multiple comparisons). For S2, significant differences remained in all five bands ($p < 0.05$; Mann-Whitney-U test, Benjamini-Hochberg correction for multiple comparisons). So, despite the effect of stimulation on the spectral power of cortical recordings, these significant differences in the bands under consideration suggest that movement detection during

stimulation will be possible.

Next, I examined tremor detection using cortical data when stimulation was enabled. Again, a binary classifier was trained and tested in the same manner as with stimulation off. Although tremor detection was not as robust as with stimulation off, the classifiers were able to reliably differentiate between periods of movement and rest (Figure 3.2B). For S1, accuracy and sensitivity were 65.4% and 82.6%, respectively, when optimized for accuracy, and 65.1% and 83.1%, respectively, when optimized for sensitivity (Table 3.2). For S2, accuracy and sensitivity were 80.5% and 94.2%, respectively, when optimized for accuracy, and 80.0% and 94.7%, respectively, when optimized for sensitivity (Table 3.2).

The results presented thus far show that tremor-inducing movement can be reliably detected from neural signals recorded from cortical areas, both during stimulation and when stimulation is off. However, optimizing the methods and models for tremor detection has not yet been discussed. So far, tremor detection has been investigated using a simple linear classifier with features extracted using a 1-second window. This classifier was trained using about four minutes of data, with long movement periods (30 seconds) interspersed by rest periods of a similar duration. However, several of these design choices can be altered to try to improve detection. Therefore, I altered the "chunking" window length and the lengths of movements in the prompted movement task to investigate their effects on tremor detection.

First, "chunk" window length was varied to two seconds. Features were extracted using Welch's method with a 1-second Hann window and 50% overlap. This method of PSD estimation yields the same number of features as the periodogram method did above, and only power between 4-30 Hz was used as features for the classifier. The performance of this system using 2-second chunks can be seen in Table 3.2. For S1, this change categorically improved tremor detection when compared to using 1-second chunks when stimulation was both off and on. For S2, using 2-second chunks had different effects, mostly decreasing performance when stimulation was off and increasing performance when stimulation was on.

Next, the nature of the prompted movement task was varied. Instead of only 4-5 relatively long movement and rest periods (denoted "LONG"), the task consisted of shorter rests and movements whose lengths were drawn from a uniform distribution from 3 to 12 seconds (denoted "SHORT"), for a total of approximately 16 movement periods (Figure 3.2C). For both S1 and S2, movement detection when stimulation was off was better using "LONG" movement task data compared to using "SHORT" data. However, when stimulation was on, movement detection

was better using "SHORT" movement task data for both subjects. Additionally, as with the "LONG" movement task, the "chunk" window length for creating features was also varied from 1-2 seconds using the data recorded during the "SHORT" movement task. Using a two-second window did not have a general effect in all cases, but the specific effects when using different combinations of parameters can be seen in Table 3.2.

Up to this point, all results have been derived from data from a single visit for each subject. As with signals recorded from deep brain structures in chapter 2, it would be useful to have an idea of how stable the signals are over long time periods (i.e. months to years). To gain insight into this question, cortical signals recorded during prompted movement tasks over a span of several months were examined (eight months for S1, four months for S2). For both subjects, spectra during rest and movement were remarkably consistent across the time period being examined (Figure 3.3A). For subject S1, during almost the entire span, there were significant differences in all five frequency bins (4-8 Hz, 8-12 Hz, 12-20 Hz, 20-30 Hz, 30-50 Hz; $p < 0.05$; Mann-Whitney-U test with Benjamini-Hochberg correction for multiple comparisons). For S2, there also consistent significant differences in almost all frequency bins (4-8 Hz, 8-12 Hz, 12-20 Hz, 20-30 Hz, 30-50 Hz; $p < 0.05$; Mann-Whitney-U test with Benjamini-Hochberg correction for multiple comparisons).

Using cortical data from the movement prompt task recorded during an initial visit (0 month for S1, 2 month for S2; data were recorded during month 0 visit for S2 at a lower sampling rate and therefore was not suitable for classifier training) for a given subject, two classifiers were trained; one optimized for accuracy, the other for sensitivity. These classifiers were then used to predict movement from cortical data recorded during the movement prompt task in subsequent visits for that subject. For all visits for both subjects, classifier performance was significantly greater than chance ($p < 0.01$; McNemar's test), and scores ranged from 70%-95% up to eight months after classifier training (Figure 3.4).

3.4 Discussion

This work presented in this chapter aimed to address the question: can essential tremor be reliably detected from neural signals recorded from cortical areas using a chronically-implanted DBS system, and if so, is this detection better than detection using signals from deep-brain structures? To answer this question, cortical recordings from two ET subjects performing a

Table 3.2: Classifier performance

	Parameters			**Opt. Accuracy**		**Opt. Sensitivity**	
Subject	Stim OFF/ON	Win. Len.	Training Periods	Acc.	Sens.	Acc.	Sens.
S1	OFF	1	LONG	75.7%	92.9%	75.5%	93.4%
S1	OFF	2	LONG	**83.2%**	**94.7%**	**82.9%**	**96.8%**
S1	OFF	1	SHORT	66.3%	84.2%	66.2%	84.5%
S1	OFF	2	SHORT	68.5%	79.9%	68.5%	79.9%
S1	ON	1	LONG	65.4%	82.6%	65.1%	83.1%
S1	ON	2	LONG	68.0%	84.5%	67.9%	85.4%
S1	ON	1	SHORT	70.1%	**91.9%**	70.1%	**91.9%**
S1	ON	2	SHORT	**73.0%**	89.9%	**72.5%**	91.3%
S2	OFF	1	LONG	**90.6%**	**92.5%**	89.1%	**95.9%**
S2	OFF	2	LONG	92.0%	92.1%	**91.8%**	94.9%
S2	OFF	1	SHORT	86.5%	92.3%	86.2%	93.0%
S2	OFF	2	SHORT	83.0%	88.4%	81.6%	88.8%
S2	ON	1	LONG	80.5%	94.2%	80.0%	94.7%
S2	ON	2	LONG	83.9%	94.0%	83.9%	94.0%
S2	ON	1	SHORT	**85.6%**	**94.9%**	**84.3%**	**95.3%**
S2	ON	2	SHORT	85.2%	91.2%	82.5%	91.8%

prompted movement task meant to induce tremor were analyzed. First, spectral power during rest and movement were examined under both off-stimulation and on-stimulation conditions. Large, statistically significant decreases in power across alpha-beta frequency bands (8-30 Hz) were observed during movement in both subjects, in line with what has been observed in motor ECoG recordings in patients with essential tremor [2][5][11] and other movement disorders [10]. Desynchronization was also occasionally observed in the low-gamma frequency range (30-50 Hz), which is opposite in sign of the reported increases in power in this band typically associated with movement [8]. However, at least one other study has reported seeing this unexpected decrease in low-gamma power during movement in Parkinson's disease [10]. The authors of that study suggest that this decrease in low-gamma power during tremor reflects a physiological difference in neural activity between tremor and normal movement. This hypothesis is supported by spectra observed during stimulation; although there is still a significant decrease in

low-gamma power during movement (without tremor), the change is much smaller in amplitude and likely dominated by the power differences in frequencies around 30 Hz. Therapeutic stimulation reduced power in several frequency bands, with the largest effect on beta-band power, during both movement and rest. This stimulation-induced beta-band desynchronization is a documented effect in both Parkinson's disease and essential tremor [12].

During stimulation, movement still resulted in significant broadband desynchronization for subject S2, but for S1, significant differences were localized only to theta (4-8 Hz) and low-beta (20-30 Hz). One explanation for this discrepancy between subjects is the physical movement performed during the task and the effect of therapeutic stimulation on that movement. For subject S1, the movement consisted of holding his right hand approximately one inch from his chin with his index finger extended. With stimulation disabled, maintaining this posture reliably evoked tremor. However, with stimulation enabled, tremor disappeared and no movement was observed. The subsequent isotonic contractions for maintaing the arm/hand posture likely did not evoke as much desynchronization as continuous movement might [7]. For subject S2, although stimulation reduced or eliminated tremor, the movement task required more effort and resulted in more movement, likely causing greater desynchronization.

Next, binary classifiers were trained using features derived from the cortical signals recorded during the prompted movement task. The classifiers were then used to detect tremor-inducing movement, under conditions of therapeutic stimulation being both off and on. The length of movement periods during the prompted movement task and the sliding window length used for generating features were both varied to examine their effect on movement detection. For all classifiers under all conditions, accuracy and sensitivity ranged from 65% to 95%. In general, movement detection was more accurate with stimulation off compared to stimulation on. This difference in performance during therapeutic stimulation is expected, given its non-trivial effect of compressing movement and rest power (i.e. decreasing the difference between the two) in the frequency bands being used as features for classification, as mentioned above.

For both subjects, classifier performance varied for the different movement tasks used ("LONG" vs "SHORT"), but generally, performance with stimulation enabled was higher during the "SHORT" task than during the "LONG" task, and performance with stimulation disabled was opposite. As discussed above, when stimulation is on, tremor is largely absent while the subjects are maintaining their movement position. This absence of continuous movement results in less desynchronization, but during the "SHORT" task, a higher proportion of the "move-

ment" actually consists of movements, rather than just maintaining a position, resulting in larger desynchronization and thus better classification. With stimulation off, the long, relatively few, movement periods in the "LONG" task result in fewer initiations/cessations of movement, which have more muddled spectral signatures than time points taken in the middle of movement (due to the 1/2 second sliding window). Therefore, the higher occurrence of movement initiations/cessations in the "SHORT" task with stimulation off may make it more difficult for the classifier to distinguish between rest and movement and decrease performance. The effect of using a one- or two-second sliding window for calculating PSD was not consistent and depended on the other conditions (stimulation off/on, "SHORT"/"LONG", etc.).

For all combinations of stimulation, movement task, and sliding window length, two separate classifiers were trained; one was optimized for accuracy and the other was optimized for sensitivity (true positive rate, recall). This was done to reflect the choices that must be made in developing an actual closed-loop DBS system. In the case of essential tremor overall accuracy may not be the best metric to optimize. Currently, continuously-delivered stimulation effectively has a 100% false positive rate since it is always on, whether the user is experiencing tremor or not. Therefore, any reduction in the false positive rate would be better in this regard than current stimulation paradigms. Because accuracy penalizes false positives, it may be better to use sensitivity as an optimization metric, which only penalizes false negatives. Using sensitivity to optimize classifiers thus results in fewer false negatives, which equates with the system missing fewer instances of tremor. Future systems may be able to take user preferences into account, and switch between optimizing for accuracy (overall detection of rest/tremor) and sensitivity (prioritized detection of tremor at the cost of occasional false positives).

While this is the first time machine learning has been used to detect tremor-inducing movement from cortical signals in ET, other studies have used features derived from ECoG signals to decode movement for brain-computer interfaces. Many of these studies have been able to achieve high performance in tasks such as classifying different finger movements from rest (97%) [1]. However, almost all of the studies of this type have used ECoG grids with dozens of contacts spanning large areas of motor cortex. It is remarkable that the movement detection obtained herein has only used a single channel of cortical data.

It should be noted that this study relied on the logistic regression classifier for tremor detection. This is a linear classifier that resides far on the simple side of the model complexity spectrum. It is reasonable to suppose that more complex, non-linear classifiers may be able

to achieve better performance. To address the issue of model complexity perhaps not being sufficient to effectively distinguish between tremor and rest spectra, the same classifier analysis as described above was performed for a non-linear classifier, the support vector machine (SVM). Using a radial basis function to create non-linear features, the SVM can fit more complex data, and potentially increase tremor detection. Substituting SVM for logistic regression, however, had little effect on accuracy and sensitivity when optimizing for accuracy; for the majority of parameter/training data combinations, accuracy either increased or decreased by 1-2%, although sensitivity did increase up to 5-6% for some parameter combinations. When optimizing for sensitivity, the classifiers always achieved 100% sensitivity by creating a trivial model that simply always predicts tremor, regardless of the features inputted. This trivial model is essentially what continuous DBS already achieves, so it would be useless for CLDBS. These results suggest that while more complex models can incrementally increase tremor detection, simple linear models seem to perform adequately. This, together with their low computational complexity, make them promising for use in low-power, embedded closed-loop systems.

The aim of the work presented in this chapter was to determine if tremor detection is possible using cortical signals, and if so, if detection is better using cortical signals or deep signals. The results presented show that tremor detection is indeed possible using cortical signals, answering the first part of the aim. In chapter 2, tremor detection with VIM signals using the same methods described in this chapter yielded accuracy and sensitivity values of 61.2% and 71.4% for subject S1, and values of 68.4% and 78.0% for subject S2 (optimizing for accuracy; values when optimizing for sensitivity were similar). When using cortical signals, these metrics became 75.7% and 92.9% for subject S1 and 90.6% and 92.5% for subject S2. So, using cortical signals yielded a 15-30% rise in classifier performance. It should be noted that movement detection from VIM signals during stimulation was not even feasible, making a comparison under these conditions impossible. Taken together, these results show that cortical signals are a better candidate for tremor detection than deep brain signals, at least from the VIM for essential tremor. This disparity between classifier performance using the different signal sources comes as no surprise given the potential downfalls to sensing from DBS electrodes outlined in the discussion section of chapter 2, as well as the benefits to cortical sensing presented in the introduction section to this chapter.

It should be noted that this work made no attempts at distinguishing tremor-inducing movements from non-tremor inducing movements. While this would be important and useful in

future iterations of the closed-loop system, current hardware limits the ability to do so. Only a single channel of data can be sensed at a time, making the detection of spatially-restricted changes in neural activity that are highly correlated with different movements, such as changes in gamma band activity, unfeasible.

3.5 Summary

In this chapter, I presented data collected from two subjects with essential tremor who had been implanted with a DBS system and an electrocorticography electrode over motor and somatosensory cortex. Cortical signals were collected while the subjects engaged in various prompted movement tasks, with stimulation both enabled and disabled. I found that there were significant differences in power in several frequency bands with stimulation both on and off, even though stimulation had a broadband reducing effect on spectral power. I also trained classifiers to detect tremor-inducing movement using these cortical data, and examined their performance. Movement was detected with accuracies up to 92%, far outperforming detection using deep brain signals. Lastly, I examined tremor detection when classifiers were trained during one visit and used to detect tremor up to 8 months later, showing that sensed neural activity, and consequently, movement detection, is consistent over extended periods of time.

References

[1] C. A. Chestek, V. Gilja, C. H. Blabe, B. L. Foster, K. V. Shenoy, J. Parvizi, and J. M. Henderson, "Hand posture classification using electrocorticography signals in the gamma band over human sensorimotor brain areas.," *Journal of neural engineering*, vol. 10, no. 2, p. 026 002, 2013.

[2] A. L. Crowell, E. S. Ryapolova-webb, J. L. Ostrem, N. B. Galifianakis, S. Shimamoto, D. A. Lim, and P. A. Starr, "Oscillations in sensorimotor cortex in movement disorders : an electrocorticography study," *BRAIN*, 2012.

[3] A. D. Degenhart, J. Eles, R. Dum, J. L. Mischel, I. Smalianchuk, B. Endler, R. C. Ashmore, E. C. Tyler-Kabara, N. G. Hatsopoulos, W. Wang, A. P. Batista, and X. T. Cui, "Histological evaluation of a chronically- implanted electrocorticographic electrode grid in a non-human primate," *Journal of Neural Engineering*, vol. 13, 2016.

[4] J. A. Herron, M. C. Thompson, T. Brown, H. J. Chizeck, J. G. Ojemann, and A. L. Ko, "Chronic electrocorticography for sensing movement intention and closed-loop deep brain stimulation with wearable sensors in an essential tremor patient," *Journal of Neurosurgery*, pp. 1–8, 2016.

[5] E. D. Kondylis, M. J. Randazzo, A. Alhourani, W. J. Lipski, T. A. Wozny, Y. Pandya, A. S. Ghuman, R. S. Turner, D. J. Crammond, and R. M. Richardson, "Movement-related dynamics of cortical oscillations in Parkinson ' s disease and essential tremor," pp. 1–13, 2016.

[6] E. C. Leuthardt, G. Schalk, J. R. Wolpaw, J. G. Ojemann, and D. W. Moran, "A brain-computer interface using electrocorticographic signals in humans.," *Journal of neural engineering*, vol. 1, no. 2, pp. 63–71, 2004.

[7] K. Nakayashiki, M. Saeki, Y. Takata, Y. Hayashi, and T. Kondo, "Modulation of event-related desynchronization during kinematic and kinetic hand movements," *Journal of NeuroEngineering and Rehabilitation*, vol. 11, no. 1, p. 90, 2014.

[8] G. Pfurtscheller, B. Graimann, J. E. Huggins, S. P. Levine, and L. A. Schuh, "Spatiotemporal patterns of beta desynchronization and gamma synchronization in corticographic data during self-paced movement," *Clinical Neurophysiology*, vol. 114, pp. 1226–1236, 2003.

[9] G. Pfurtscheller and F. L. da Silva, "Event-related eeg/meg synchronization and desynchronization: Basic principles," *Clinical Neurophysiology*, vol. 110, no. 11, pp. 1842–1857, 1999.

[10] S. E. Qasim, C. de Hemptinne, N. C. Swann, S. Miocinovic, J. L. Ostrem, and P. A. Starr, "Electrocorticography reveals beta desynchronization in the basal ganglia-cortical loop during rest tremor in Parkinson's disease," *Neurobiology of Disease*, vol. 86, pp. 177–186, 2015.

[11] N. C. Rowland, C. D. Hemptinne, N. C. Swann, S. Qasim, S. Miocinovic, J. L. Ostrem, R. T. Knight, and P. A. Starr, "Task-related activity in sensorimotor cortex in Parkinson ' s disease and essential tremor : changes in beta and gamma bands," *Frontiers in Human Neuroscience*, vol. 9, no. September, pp. 1–12, 2015.

[12] D. Whitmer, C. de Solages, B. Hill, H. Yu, J. M. Henderson, and H. Bronte-Stewart, "High frequency deep brain stimulation attenuates subthalamic and cortical rhythms in Parkinson's disease.," *Frontiers in human neuroscience*, vol. 6, no. June, p. 155, 2012.

Chapter 4

Closed-loop Stimulation for Essential Tremor

4.1 Introduction

This chapter presents work done to address Aim 3 of this dissertation: **develop and test the performance of a closed-loop system for mitigating essential tremor that uses neural activity as a biofeedback signal**. The previous two chapters have examined neural signals acquired from deep brain structures and cortical areas in subjects with ET. The results of these chapters demonstrated that cortical signals obtained from an ECoG electrode implanted with a DBS system are superior for detecting tremor-inducing movement than signals acquired from DBS electrodes, and that they can be used to detect movement with a high degree of accuracy. Importantly, chapter 3 demonstrated that movements can be detected reliably from cortical signals, even in presence of stimulation. These results suggest that it will be possible to use cortical signals to detect movement and alter stimulation parameters to mitigate tremor in real-time.

To date, there has only been a single example of closed-loop control of DBS using a neural signal, which was done in PD patients [6]. This study used beta-band (12-30 Hz) power from STN recordings to trigger stimulation, with promising results. Specifically, the algorithm used manually-tuned thresholds for beta-band power to detect symptoms. This method of training the closed-loop system would be onerous for clinicians and/or patients to program, and would not make use of power in other frequency bands known to have symptom-related changes, such as tremor band (4-8 Hz, typically). A better approach would be to use machine learning to

automatically determine which neural features are most correlated with movement and build a patient-specific model relating the two. Machine learning has been used to detect symptoms in neural signals recorded from movement disorder patients with great success [2][1][3][7][9]. However, all of the aforementioned studies only used machine learning to detect symptoms offline, that is, from previously recorded data, and therefore did not use the symptom detection from these models to actually alter stimulation. Therefore, using machine learning to detect symptoms from neural data and alter stimulation in real-time remains to be done.

Also, in [6], experiments were done peri-operatively, and did not make use of chronically-implanted DBS systems. Therefore, a crucial next step towards developing a closed-loop system that can be used in the day-to-day life of people with movement disorders is to utilize commercially-available (although possibly investigational), chronically-implanted devices for closed-loop control. Therefore, the goal of the work presented in this chapter was to develop a closed-loop DBS system that is novel in the following three aspects: 1) harnesses the power of machine learning to build patient-specific models relating neural signals and symptoms, and 2) uses chronically-implanted DBS devices and sensing electrodes and 3) uses cortical activity as a biosignal. This closed-loop system was developed and tested in ET subjects, and its performance was analyzed both on the basis of its ability to detect tremor-inducing movement and deliver stimulation at the correct time, and its therapeutic effect on symptoms.

4.2 Methods

4.2.1 Data Collection

This experiment was approved by the FDA (through an investigational device exemption) and the University of Washington IRB. For this study, two subjects diagnosed with idiopathic essential tremor were used (for subject information, see Table 4.1). Both subjects were implanted with a Medtronic Activa PC+S (Medtronic; Minneapolis, Minnesota, USA) DBS system for treatment of essential tremor. A Medtronic 3389 4-contact electrode was inserted into the left ventral intermediate nucleus (VIM) of the thalamus, and therapeutic stimulation was delivered using this electrode. Additionally, a 4-contact electocorticography strip was implanted over the hand/arm region of left motor and somatosensory cortex (Figure 4.1). The placement of the electrodes were confirmed by coregistred MRI and CT scans. Each of these electrodes can sense local field potentials from the surrounding neural tissue using two of the contacts in a

Table 4.1: Patient Information

Subject	Sex	Age	Affected Limb	Implant Side	Recording Contacts	Stimulation Contacts	DBS Settings
S1	M	58	RH	L	8-10	2+/0-	2.5V,140Hz,90µs
S2	M	81	RH	L	9-11	2+/0-	3.5V,130Hz,90µs

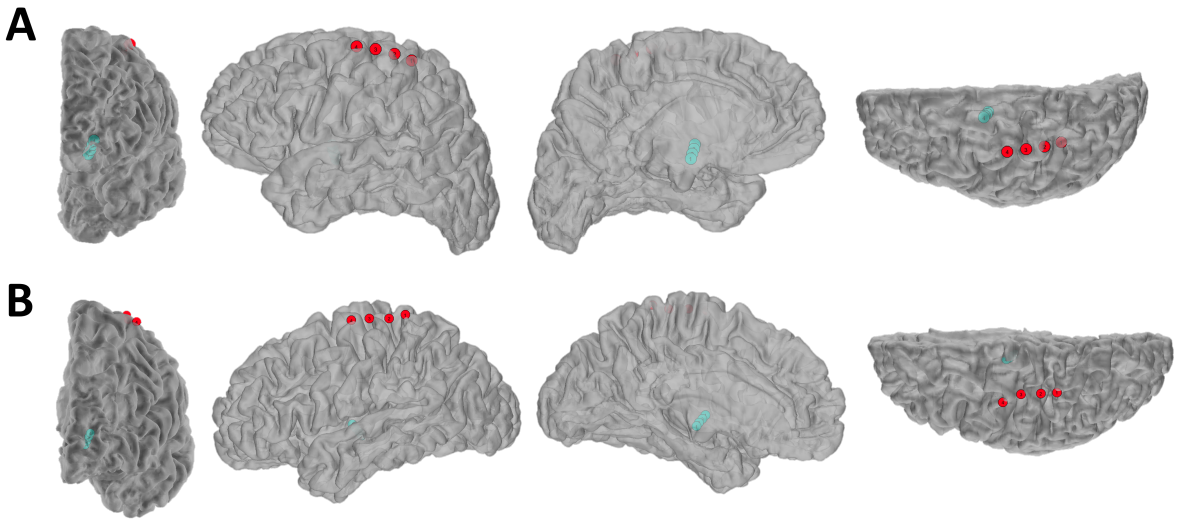

Figure 4.1: Coregistered MRI and CT scans showing cortical (red) and depth (blue) electrode placement in subject S1 (A) and S2 (B). From left to right, the view of each scan is frontal, lateral, medial and superior.

differential configuration. The DBS system thus is capable of streaming a single channel of data from each electrode and updating stimulation parameters in real-time. For this experiment, the contact pairs from each subject that provided the highest amplitude signal compared to other contact pairs on the cortical electrode were used (see Table 4.1 for specific contacts used). Neural activity was sampled at 422 Hz, low-pass filtered at 100 Hz and high-pass filtered at 0.5 Hz with a gain of 2000. In addition to neural signals, gyroscope data were collected during the experiment using a wrist-worn commercial smartwatch on the subject's right arm. Inertial data were recorded at 100 Hz. Bipolar stimulation was delivered through the VIM electrode (see Table 4.1 for specific contacts and stimulation parameters used). Custom software was used for real-time communication through the Medtronic Nexus-D device (hardware interface between implanted Activa PC+S and personal computer) [5].

For this study, the subjects first performed a prompted movement task while neural and movement signals were collected. This task consisted of a subject-specific movement with the right hand/arm that induced tremor, as verified by inspection of gyroscope data. Both subjects

were seated for the duration of the prompted movement task. For subject S1, this movement consisted of a holding his right hand just below his nose with his index finger extended (mimicking holding a utensil to his mouth). For subject S2, this movement consisted of holding his index finger extended close to a point on a wall (mimicking using a screwdriver). The duration of the tasks were about 4 minutes in length. Tasks were performed with stimulation OFF and ON. Subject S1 was in an OFF-medication state during the task, but subject S2 was taking propranolol (beta-blocker) and primidone (anti-convulsant) for treatment of ET.

4.2.2 Data Processing

After completing these tasks, features were extracted from the raw neural data in the stimulation OFF condition in the following way. Power spectral density (PSD) estimations were calculated from the cortical signal five times per second using Welch's method (50% overlap) and a half-second Hann window, yielding frequency bins with a width of approximately 2 Hz. From these estimations, frequencies between 4 and 26-28 Hz were used as features for the classifier. This frequency range was chosen because it showed the largest difference between rest and movement and because it avoided spectral peaks sometimes occurring slightly higher than these frequencies that were found to degrade classifier performance if included. Labels for the classifier were created by manually demarcating movement and movement-free periods using the wrist-worn gyroscopic sensor data. Features corrupted by packet drops during telemetry of the data from the DBS device to the computer were removed.

The remaining features and corresponding labels were split into two equal halves for cross-validation (2-fold cross-validation) to prevent model overfitting. Each of the two sets was scaled to have a mean of 0 and unit variance and used to train a logistic regression classifier with a given hyperparameter (range from 10^{-6} to 10^{5}). The trained classifier was then used to predict labels for the other data set. The hyperparameter that yielded the highest average sensitivity (true positive rate, recall; using gyroscopic labels for ground truth) for the two sets was chosen as optimal. The two feature/label data sets were then combined, and a single logistic regression classifier was then trained using the optimal hyperparameter. This process was then repeated for the stimulation ON data, yielding an OFF classifier and and ON classifier. The rationale for using separate classifiers for OFF and ON stimulation conditions was that stimulation decreases beta-band power, even when the subject is at rest. Thus using two different classifiers avoids possible false positives that could be caused by stimulation.

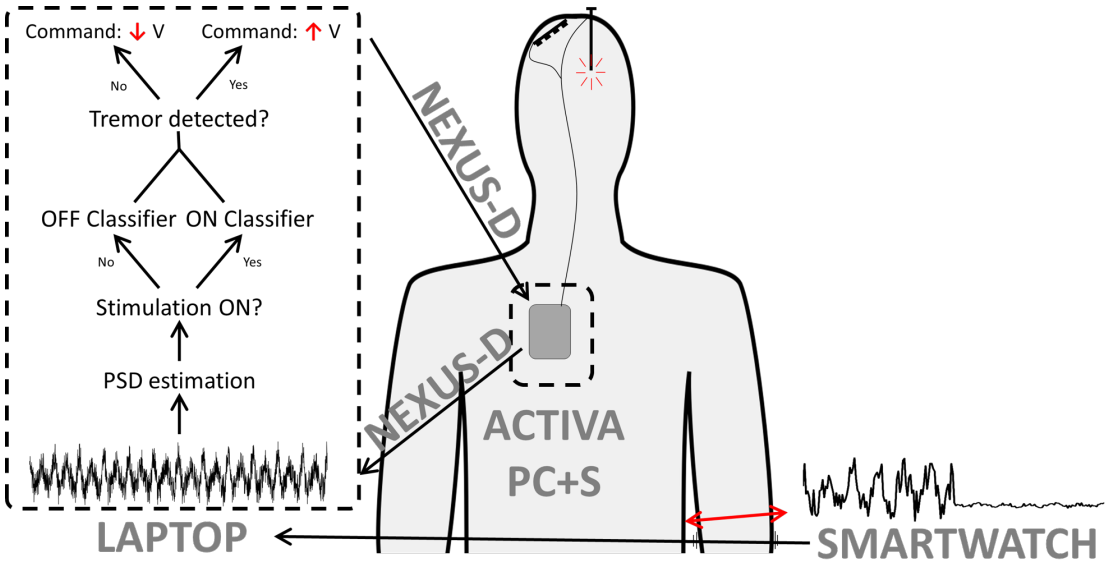

Figure 4.2: Brief description of closed-loop system. Neural activity is sampled from the cortical electrode by the Activa PC+S DBS system. These data are then wirelessly transmitted to the Nexus-D interface, which is connected via USB to a personal computer. On the computer, features are extracted from the raw neural data and then used by classifiers to determine if movement is occurring. Stimulation voltage can then be updated by sending commands back through the Nexus-D interface. Concurrently, gyroscopic information is recorded from the right arm.

4.2.3 Closed-Loop System Description

The two trained classifiers were then used in a closed-loop system to detect movement and change stimulation in real time. A description of the system can be seen in Figure 4.2. Briefly, neural data are sampled from the cortical electrode by the Activa PC+S DBS system. These data are then wirelessly transmitted through the Nexus-D every 400 ms to a personal computer running custom software for interfacing with the Nexus-D. On the computer, a chunk of neural data is used to estimate power spectral density in the 4 to 26-28 Hz range in the same manner as during the feature extraction phase of classifier training. These features are normalized and then used by the stimulation OFF/ON classifiers to determine if movement is occurring. If movement is detected, a command is sent by the Nexus-D to increase the stimulation voltage by 500 mV (not to exceed the therapeutic voltage set by the clinician). Otherwise, a command is sent to decease the stimulation voltage by 500 mV. Concurrently, gyroscopic information is recorded from the right arm. Stimulation updates are sent every 400 ms.

4.2.4 Closed-Loop Testing

After the classifiers were trained, the subjects engaged in several different tasks to examine the performance of the closed-loop system and compare it to off-stimulation and on-stimulation con-

ditions. The first task was a prompted movement task using the same movement from classifier training. For this testing task, movement and rest durations were taken from a uniform distribution in the range of 3-12 seconds. Each movement was followed by a rest period, and the total duration of the task was about four minutes (approximately 16 movements). To investigate the effect of different system design choices on system performance during the prompted movement task, several parameters of the closed-loop system were altered. First, the window length for feature extraction was varied between 1-2 seconds. The data used for training the classifiers were also varied; the "long" set had movements that were sustained for 30 seconds, interspersed by rest periods of the same length. The "short" set had movement lengths and rest lengths that were drawn from a uniform distribution from 3-12 seconds. Both the "long" and "short" data sets were approximately four minutes long. Lastly, the rule for updating stimulation was varied from decrementing voltage every time a negative classifier result (no tremor detected) was obtained to only decrementing if two consecutive negative classifier outputs were seen.

Additionally, in order to examine the performance of the system when subjects engaged in more naturalistic movements, the subject performed drawing and writing tasks used in the Fahn-Tolosa-Marin (FTM) tremor assessment [4]. The drawing task consisted of drawing a spiral and straight lines constrained by guide lines. The writing task consisted of the subject copying a one-sentence prompt.

The subjects engaged in each task using closed-loop stimulation, no stimulation (stimulation OFF) and constant stimulation at the clinical setting (stimulation ON). For the prompted movement task, the closed-loop system parameters were varied as described above. For the FTM task, only the closed-loop system using the 1-second window, trained on the "long" data were used. To quantify the performance of the closed-loop system, the accuracy and sensitivity of the pair of classifiers were calculated using the gyroscopic data as ground truth. To assess the effect of the different stimulation conditions on tremor during the prompted movement task, the mean instantaneous tremor amplitude was calculated during each prompted movement. This was accomplished by filtering each of the signals from the three gyroscopic axes with 4-order Butterworth band-pass filter centered around the subject's tremor frequency (2-Hz bandwidth). Then, the magnitude of the filtered gyroscopic signal was calculated and passed through a Hilbert transform to yield the instantaneous amplitude. The mean of this tremor envelope during each movement under a given stimulation condition was then calculated. ANOVA or Kruskal-Wallis test were used to examine group effects of stimulation condition, and correspond-

ing post-hoc tests were used to look at specific differences between stimulation conditions.

Additionally, video was recorded during the FTM tremor assessment, and symptoms were rated by two blinded clinicians for each stimulation condition.

4.3 Results

4.3.1 Closed-Loop System Performance

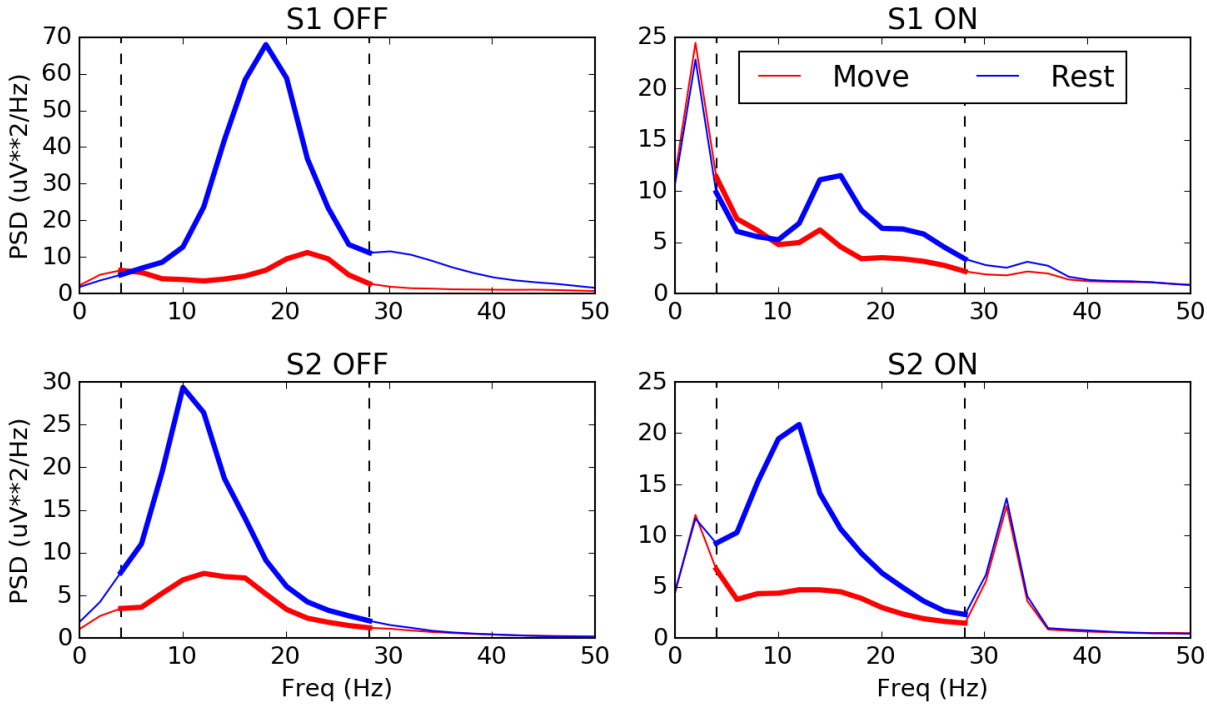

Figure 4.3: Average spectra from training data during rest (blue) and movement (red). Dashed lines show frequency bounds and bold sections of lines show frequencies used in classifiers.

Using data recorded during the prompted movement task, PSD was calculated with a sliding window and used as features for creating logistic regression classifiers. As shown in previous chapters, there were large, consistent differences in spectra during rest and movement, both with stimulation off and on, for both subjects (Figure 4.3). However, the shape of the spectra, and the differences between rest and movement spectra, were different across subjects, both in amplitude and frequency. These differences in neural activity between subjects are reflected in the coefficients for each subject's trained classifiers; the models were able to capture the unique features of each subject's neural activity (Figure 4.4).

Using the stimulation OFF and stimulation ON classifiers created with training data, each subject first engaged in a prompted movement task to assess the performance of the closed-loop

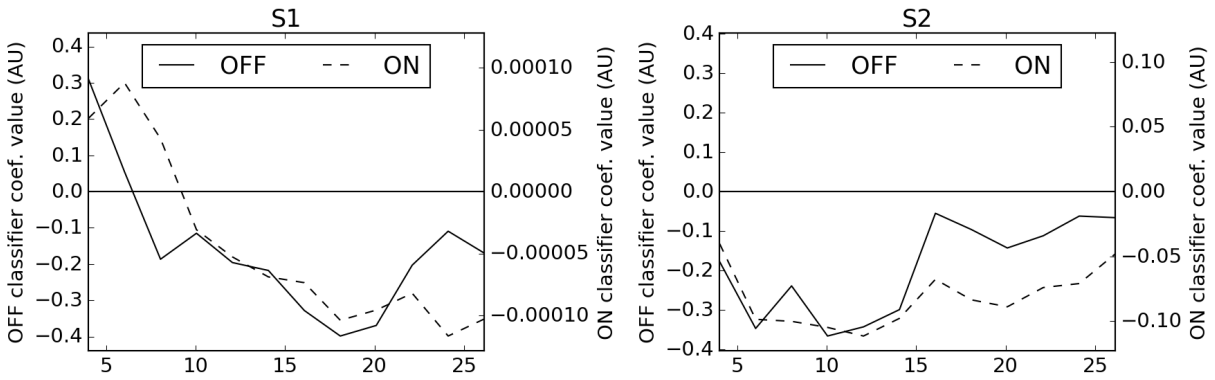

Figure 4.4: Coefficients of logistic regression classifiers trained on data with stimulation off and on ("LONG" training periods, 1-second window).

system. During this task, the classifiers detected tremor-inducing movement in real time and altered stimulation parameters accordingly (Figure 4.5A,4.5B). To quantify the performance of the system, accuracy and sensitivity were calculated using the predictions from the classifiers (Table 4.2, "1-second sliding window, long training periods"). For S1, the accuracy and sensitivity of the classifiers were 68.7% and 69.1%. For S2, the accuracy and sensitivity were 75.9% and 76.2%.

Because the system only updated the stimulation level every 400 ms and had a maximum voltage increment/decrement of 500 mV, even when the classifier had false negatives during movement, the stimulation usually did not turn off completely during a movement. Instead, the voltage was decreased by a few steps until the classifier outputted a true positive, after which the stimulation increased. Because the response of stimulation to the detection of movement was not instantaneous (i.e. requiring several steps before reaching the maximum or minimum voltage), stimulation was sometimes present even when the classifiers erroneously detected no movement. Therefore, the proportion of time for which stimulation being off or on matched the absence/presence of movement, respectively, may also be a more appropriate metric to measure the performance of the system. When using these "stimulation labels" to quantify performance, we can define accuracy (percentage of time during which stimulation off/on matched movement absent/present) and sensitivity (percentage of movement during which stimulation was on). For S1, accuracy and sensitivity using "stimulation labels" were 63.2% and 83.7%. For S2, these values were 66.8% and 87.3%. All metrics can be seen in Table 4.2.

During the prompted movement task using closed-loop control of DBS, the average stimulation voltage was 1.32 V for S1 and 2.07 V for S2. These average voltages represent a decrease of 47.4% and 41.0%, respectively, compared to each subject's therapeutic stimulation voltage (2.5

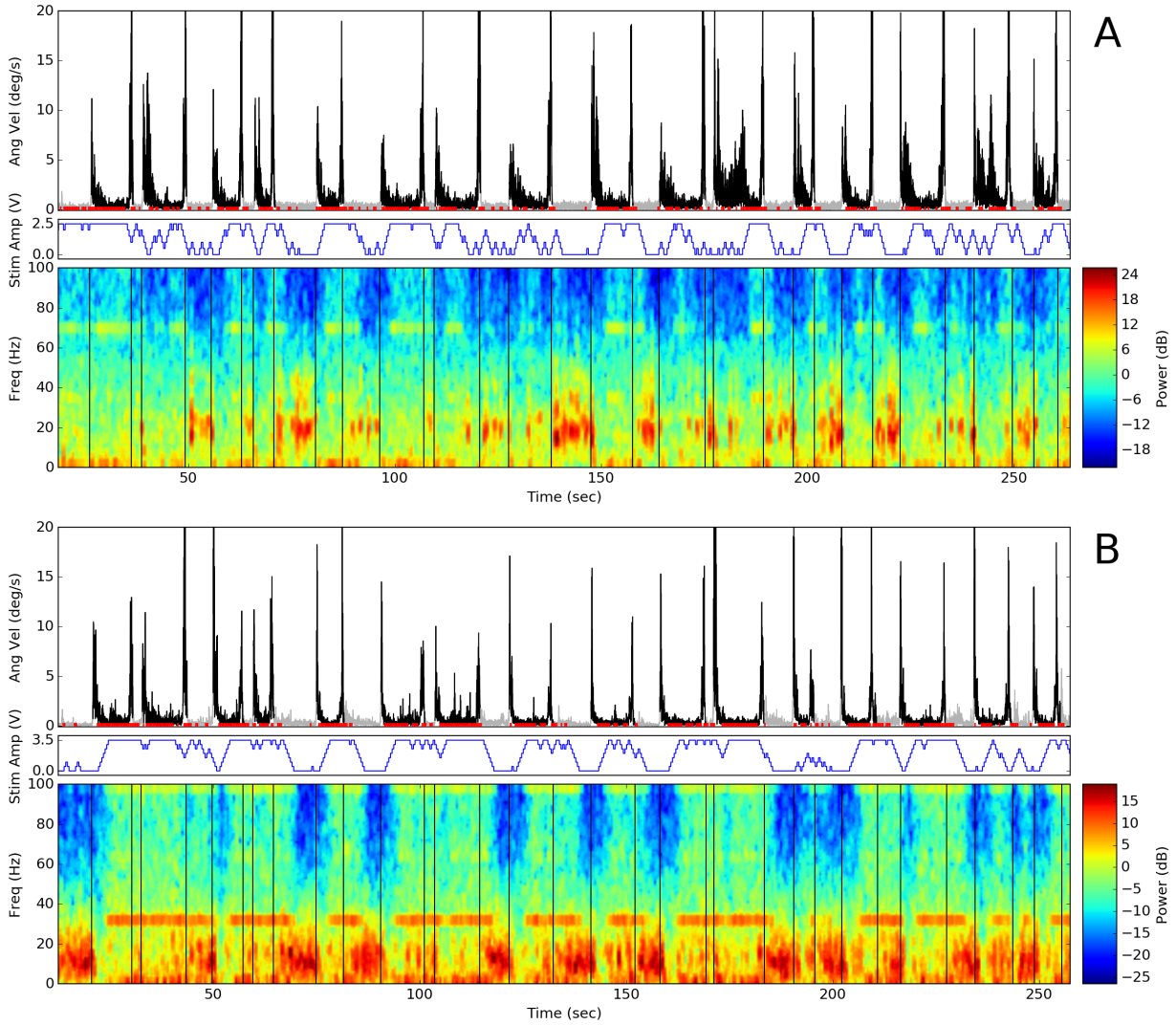

Figure 4.5: Closed-loop system performance for subject S1 (A) and S2 (B) during prompted movement task. Gyroscopic signal from right arm shows movement (black) and rest (gray) periods, along with concomitant tremor detection (red). Deep brain stimulation amplitude (blue) responds to movement detection. Spectrogram shows changes in theta (8-12 Hz) and beta (12-30) frequency bands during movement.

V and 3.5 V, respectively. Stimulation was on at some voltage (not necessarily at maximum voltage) 76.4% and 77.9% of the time, for S1 and S2, respectively. During the prompted movement task, the subjects S1 and S2 were moving 58.8%, and 59.8% of the the time, respectively, so stimulation was on more often than the subjects were actually moving. This is expected, since the classifiers were optimized for sensitivity, and because of the non-instantaneous changes in stimulation voltage. The delay between initiation of movement and the first increase in stimulation voltage was 1.36s $\pm$ 0.37s for S1 and 1.33s $\pm$ 0.59s for S2 (mean $\pm$ std, N = 12 for S1 and S2; movements which were initiated while stimulation was already on were not used).

To investigate possible design choices for optimizing the closed-loop system, several param-

Table 4.2: Prompted movement task performance

	Class. Labels		**Stim Labels**		**Stimulation**		
Subject	Acc.	Sens.	Acc.	Sens.	Avg. Voltage	Perc. Decrease	Time On
1-second sliding window, long training periods							
S1	68.7%	69.1%	63.2%	83.7%	1.32	47.4%	76.4%
S2	75.9%	76.2%	66.8%	87.3%	2.07	41.0%	77.9%
2-second sliding window, long training periods							
S1	69.7%	83.6%	62.1%	88.9%	1.70	32.1%	83.3%
S2	71.6%	69.0%	64.8%	81.7%	1.79	48.9%	73.3%
1-second sliding window, short training periods							
S1	63.8%	76.6%	57.6%	90.7%	1.77	29.3%	89.3%
S2	71.5%	68.5%	72.0%	88.2%	1.88	46.4%	76.5%
1-second sliding window, long training periods, two negative							
S1	69.4%	79.9%	61.3%	95.8%	2.01	19.8%	92.1%
S2	76.3%	78.8%	64.7%	91.8%	2.48	29.1%	86.6%

eters were altered and the prompted movement task was repeated using the altered system. First, the sliding window length used to extract PSD from the raw neural signal was varied from one second (results described above) to two seconds. This change improved performance for S1, but decreased it for S2 (Table 4.2, 2-second sliding window, long training periods). Next, the training data for the classifiers were altered. Instead of using four minutes of data with approximately 30 second movement and rest periods, four minutes of data were used with movement and rest periods drawn from $X \sim U(3, 12)$. Compared to using "long" training data, the system using "short" training data decreased accuracy but improved sensitivity for S1, and had varying effects for S2 (Table 4.2, 1-second sliding window, short training periods). Lastly, the rules used to update stimulation were altered; instead of decreasing the stimulation voltage every time a negative classifier result (no movement detected) was obtained, the system only began decreasing stimulation after two consecutive negative classifier results were found. This was done in an effort to increase the sensitivity of the system (i.e. ensure stimulation stayed on during occasional false negatives from the classifiers). As expected, this change increased the sensitivity of the system for both subjects, but also resulted in a higher average stimulation

Table 4.3: FTM task performance

	Class. Labels		**Stim Labels**		**Stimulation**		
Subject	Acc.	Sens.	Acc.	Sens.	Avg. Voltage	Perc. Decrease	Time On
Spirals							
S1	91.4%	91.4%	100.0%	100.0%	2.31	7.5%	100%
S2	87.8%	87.8%	100.0%	100.0%	3.29	5.9%	100%
Line drawing							
S1	91.9%	91.9%	100.0%	100.0%	2.45	1.9%	100%
S2	97.2%	97.2%	100.0%	100.0%	3.47	0.8%	100%
Writing							
S1	86.9%	86.9%	100.0%	100.0%	2.40	3.9%	100%
S2	85.9%	85.9%	100.0%	100.0%	3.20	8.4%	100%

amplitude and more time with stimulation on (Table 4.2, 1-second sliding window, long training periods, two negative).

Next, using the same stimulation OFF and stimulation ON classifiers as used during the prompted movement task, the subjects engaged in drawing and writing task as part of the Fahn-Tolosa-Marin (FTM) tremor assessment. These tasks were used not only to examine the therapeutic effect of closed-loop stimulation, but also to assess the performance of the closed-loop system using movements that are more representative of movements the subjects might perform during every-day activities. During the drawing/writing tasks, the closed-loop system detected movement basically the entire duration of the task, and accordingly, stimulation was on for the duration of the task in both subjects (Figure 4.6A,4.6B). The accuracy and sensitivity of the classifiers can be seen in Table 4.2. Also, as for the prompted movement task, "stimulation labels" were used to measure performance; however, because stimulation was on during the entire task, accuracy and sensitivity using "stimulation labels" were 100% (Table 4.2).

4.3.2 Clinical Effect

To assess the clinical effect of the closed-loop DBS system, subjects engaged in the FTM tremor assessment task with stimulation under closed-loop control. This task consists of various limb movements, speaking, water pouring, drawing and writing [4]. The classifiers used for movement

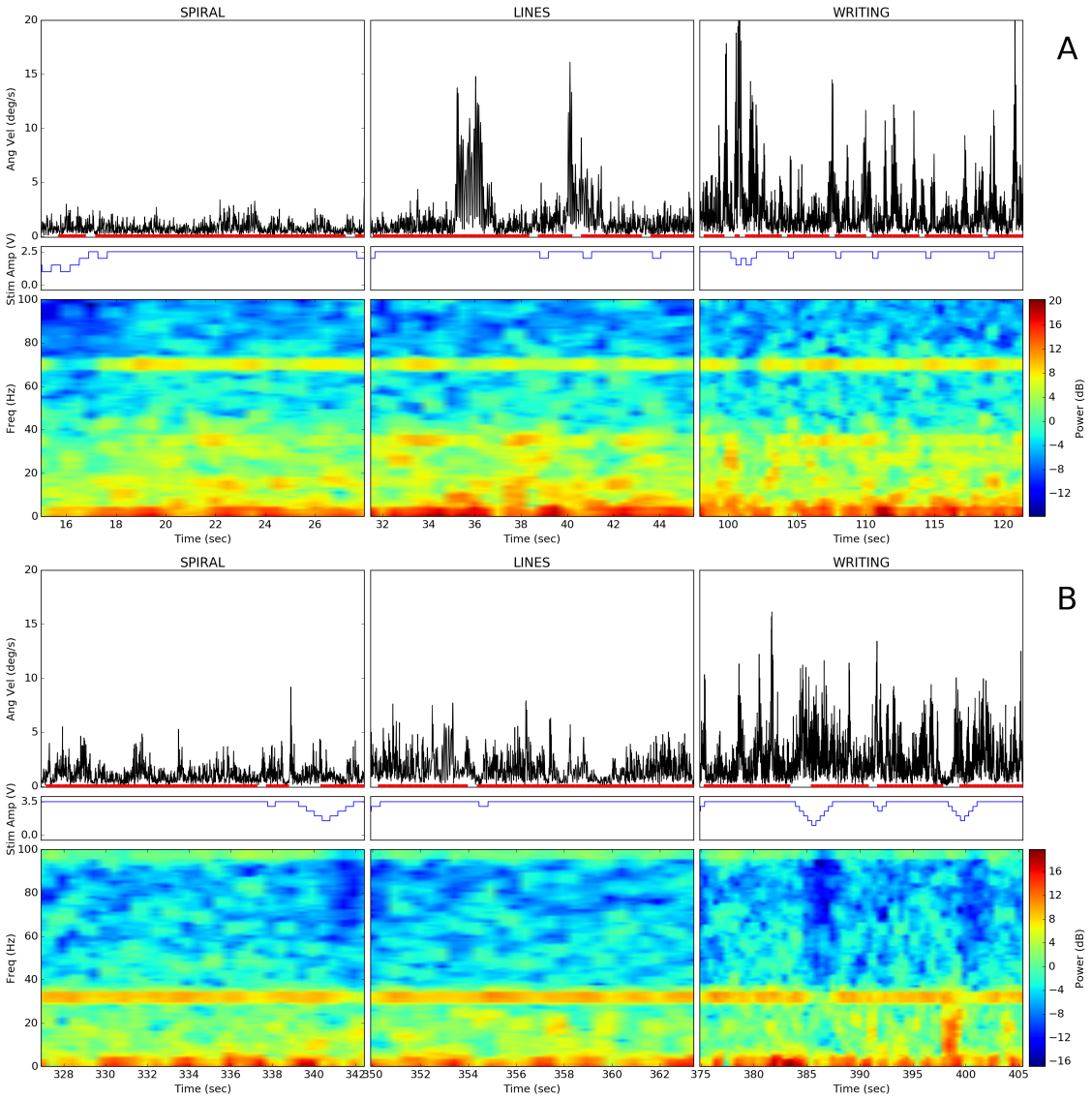

Figure 4.6: Closed-loop system performance for subject S1 (A) and S2 (B) during drawing and writing tasks. Gyroscopic signal from right arm shows movement (black), along with concomitant tremor detection (red). Deep brain stimulation amplitude (blue) responds to movement detection. Spectrogram shows absence of theta (8-12 Hz) and beta (12-30) frequency bands during movement.

detection during the FTM task were those trained with data from the prompted movement task (1-second window, "long" training periods). For comparison, subjects also engaged in the FTM assessment with stimulation turned off and with stimulation turned on at the therapeutic voltage (see Table 4.1). Video recordings were made of the subjects performing the tasks involved in the FTM assessment, and two blinded clinicians scored the severity of the tremor.

For both subjects, closed-loop DBS resulted in improved motor scores compared to both off-stimulation and on-stimulation (Table 4.4)). For S1 and S2, closed-loop DBS decreased average total scores by 48.7% and 31.1%, respectively, compared to off-stimulation, and by 16.7% and 22.5%, respectively, compared to on-stimulation. To further examine the therapeutic effect of

Table 4.4: Subscores on FTM tasks

	Subject S1			Subject S2		
Subset	**OFF**	**ON**	**CL**	**OFF**	**ON**	**CL**
Axial	2.5	1.5	0.5	2	2	2.5
Speaking	1.5	0	0.5	0.5	0.5	1
Handwriting	1	1	1	1	1	1
Left Side	5	5.5	4.5	10.5	9	7
Right Side	9.5	4	3.5	8.5	7.5	4
TOTAL	19.5	12	10	22.5	20	15.5

closed-loop DBS compared to the other stimulation conditions, scores were subdivided into axial (trunk, voice, head), left body side, right body side, speaking and handwriting categories. The most consistent improvements across subjects between on-stimulation and closed-loop DBS were in both left body side and right body side movements. These movements were both postural (maintaining a position, e.g. arms extended with palms facing down) and dynamic (moving hand between nose and target) and performed with both upper extremities and lower extremities. Examples of the spiral and line drawings made by the subjects during the tremor assessment task under the different stimulation conditions can be seen in Figure 4.7 and Figure 4.8, respectively.

To further assess the therapeutic effect of closed-loop DBS and compare in off-stimulation and on-stimulation, mean tremor amplitudes during each movement in the prompted movement task were calculated for each stimulation condition. For subject S1, stimulation had a significant group effect on mean tremor amplitude ($p < 0.01$, Kruskal-Wallis H-test; Figure 4.9). Post-hoc analyses showed a significant decrease in tremor amplitude between off-stimulation and on-stimulation conditions, as well as a significant decrease in tremor amplitude between off-stimulation and closed-loop DBS conditions ($p < 0.01$, $p < 0.05$, respectively; Mann-Whitney-Wilcoxon test). For subject S2, however, stimulation had no group effect on tremor amplitude (Figure 4.9).

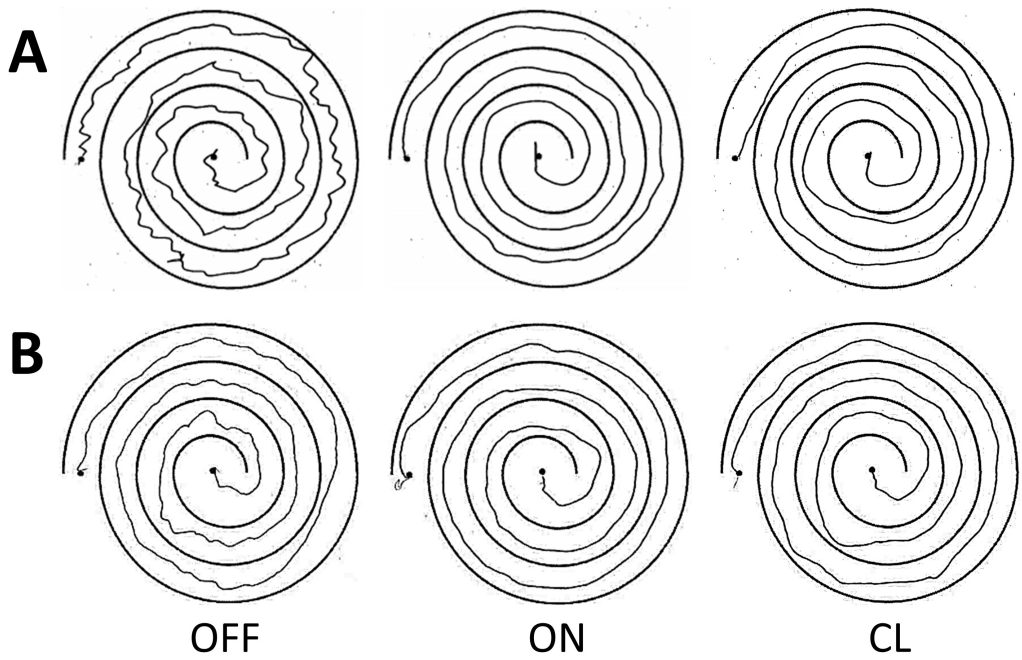

Figure 4.7: Spirals drawn by subject S1 (A) and S2 (B) as part of the FTM tremor assessment task.

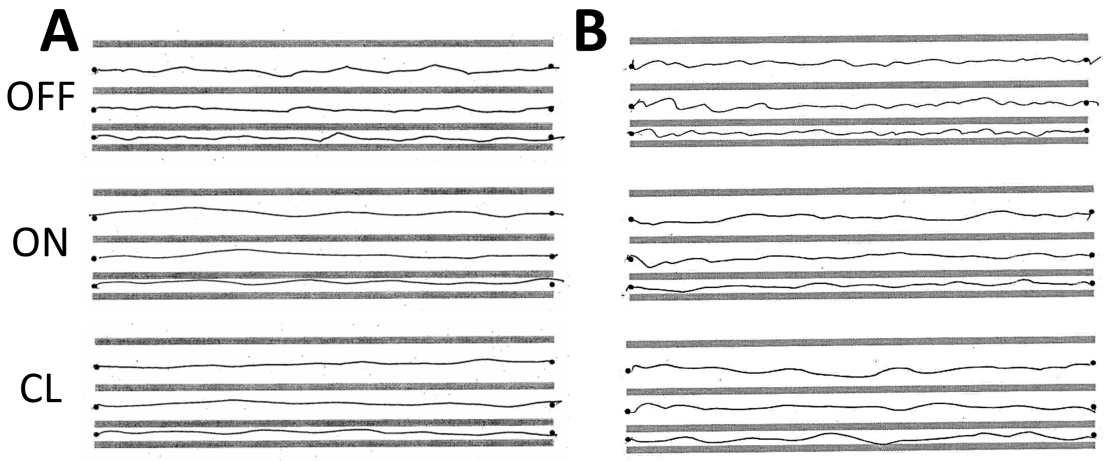

Figure 4.8: Lines drawn by subject S1 (A) and S2 (B) as part of the FTM tremor assessment task.

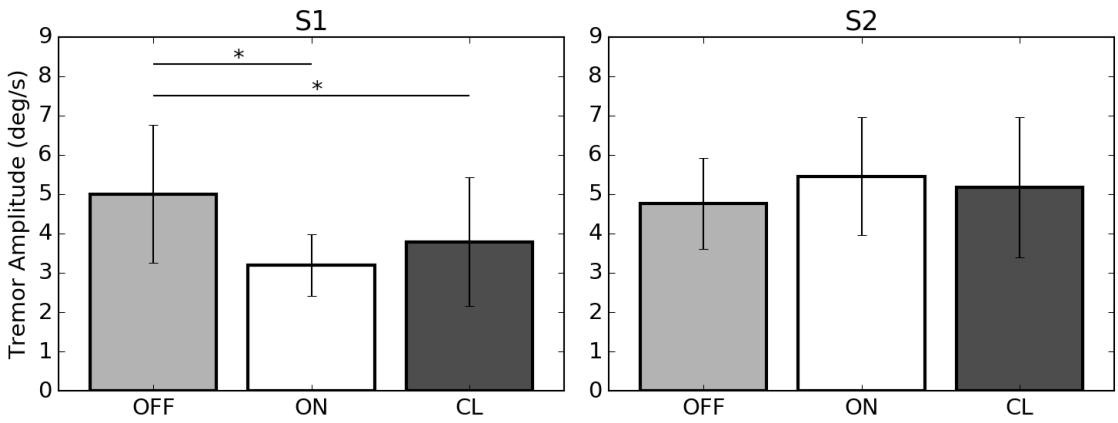

Figure 4.9: Tremor amplitude during prompted movement task. Bars show the grand average of tremor amplitude during each movement ± the standard deviation. For subject S1, tremor amplitude was significantly decreased during closed-loop stimulation and continuous stimulation ($p < 0.05$; Mann-Whitney-Wilcoxon test). For subject S2, there were no significant differences in tremor amplitude between conditions.

4.4 Discussion

The purpose of the work presented in this chapter was to address aim 3 of this dissertation, which was to develop and test the performance of a neural biofeedback signal-based, closed-loop system for mitigating essential tremor. Previous chapters examined the ability to detect tremor-inducing movement using VIM signals (chapter 2) and cortical signals (chapter 3) in ET subjects, and the results from these two chapters showed that cortical signals were superior for use in movement detection. Therefore, to address this aim, cortical signals were used as biosignal for tremor-inducing movement detection.

Evaluation of the capabilities of the closed-loop system fell into two categories. The first category was system performance, which included the ability of system to accurately detect movement and deliver stimulation when detected, the delay with which the system responded to movement detection, and the power savings achieved by not stimulating during rest. The second category was therapeutic effect, which consisted of the ability of the closed-loop system to ameliorate the symptoms of ET in satisfactory way.

The performance of the system was first evaluated with a prompted movement task using a repeated movement that evoked tremor (in the absence of stimulation). For both subjects, the system of classifiers had an accuracy between approximately 65-75%, depending on the different system design choices made. However, accuracy may not be the best metric for evaluating the performance of the system because it penalizes false negatives (movement occurring but not detected) as much as false positives (movement detected, but not actually occurring). For most

DBS patients, it is likely to be preferable to penalize false negatives more than false positives (better to occasionally stimulate during rest than not stimulate during movement). Therefore, the sensitivity (true positive rate, recall) of the system may be a more appropriate metric since it only penalizes false negatives. For both subjects, the classifiers typically had a sensitivity metric between 70-85%.

Also, as mentioned in the results section, the non-instantaneous response of the stimulation to movement detection meant that stimulation was occasionally on even though a false negative had been outputted from the classifier. Therefore, "stimulation labels" can be used instead of classifier labels to measure performance. Using these "stimulation labels", the sensitivity of the system (now meaning the percentage of time that stimulation was on during movement) was typically 80-95%, depending on the system design parameters. So, the system was delivering stimulation the vast majority of the time that the subjects were engaging in the prompted movements.

Several system parameters were varied in an attempt to optimize the system. The first of these parameters was the sliding window length used to extract features by calculating power spectral density (PSD). Because the PSD estimation method used was Welch's method, the variance of the PSD estimate decreases as more data are used (given a constant segment length), which is desirable for optimal classifier performance. However, there are several drawbacks to using long sliding windows. First, longer windows will cause proportionally more data points that overlap between movement and rest. Because of the large differences in spectral content during these two phenomena, stationarity assumptions important to the PSD calculation are more likely to be violated, resulting in poor PSD estimates. A second, and related issue, is that longer sliding windows can cause longer delays in the closed-loop system. It is desirable that stimulation reacts very quickly when movement is detected so that tremor can be ameliorated as soon as possible.

The second parameter that was varied was the length of movement and rest periods in the prompted movement training task. The "long" periods training set had movement and rest periods that were approximately 30 seconds in duration and were meant to provide few transitions between movement and rest, which decrease the quality of PSD estimates. The "short" periods training set had movement and rest periods that were between 3-12 seconds, which were meant to simulate the duration of more normal movements.

The third parameter that was varied was the control policy used to change stimulation when

movement was or was not detected. Because the method used for detecting tremor was a binary classifier, some control schemes, such as increasing stimulation in proportion to the severity of the tremor, were not possible. However, a parameter that could be adjusted was the number of positive or negative classifier predictions before a control decision is made. Again, as with sliding window length, there are trade offs in optimizing this parameter. Requiring a fixed number of consecutive positive or negative predictions before making a control decision would effectively average out false positives and negatives and make the control more accurate. However, because new data is only available every 400 ms, using multiple predictions could result in large delays in the system. Additionally, the control policies for increasing and decreasing stimulation do not need to be the same.

Varying these three parameters did not have a consistent effect across subjects and metrics for the most part. Longer sliding windows lengths were generally better for S1 and generally worse for S2, and short training periods improved sensitivity in S1, but worsened other metrics. These results seem to be in line with those found when varying parameters in chapter 3, where sliding window length and movement/rest period length also did not have a consistent effect, and suggest that these parameters will likely need to be optimized on a patient-by-patient basis. However, the one parameter that did have a consistent effect was using two negative classifier outputs instead of one to trigger stimulation decreases. Unsurprisingly, this resulted in a much higher "stimulation label" sensitivity i.e. stimulation was on more frequently during movement (92-95% of the time). However, this increase in sensitivity was accompanied by an increase in average stimulation voltage, so using two negative outputs before decreasing stimulation would favor optimizing therapy over power consumption.

Subjects also engaged in writing and drawing tasks as part of the FTM tremor assessment, and performance of the system was examined using these more natural movements. The classifiers were more accurate at detecting movement and rest during these tasks than the prompted movement tasks, achieving accuracies of 85-97%. As with the prompted movement task, "stimulation labels" can also be used to measure performance. For both subjects, there were few enough false negatives from the classifiers that stimulation actually remained on at some voltage (not necessarily the maximum) the entire duration of the drawing and writing tasks, achieving an "stimulation label" accuracy and sensitivity of 100% (accuracy was also 100% because the subjects were moving for entire duration of the drawing and writing tasks). A likely reason for the improved performance during the drawing/writing tasks compared to the prompted movement

task is that the drawing/writing tasks entailed continuous motion, resulting in more robust and/or continuous changes in in neural activity. The prompted movement tasks, on the other hand, involved the subjects maintaining a given position with the affected limb. With stimulation off, this resulted in tremor, so continuous motion was present. However, during stimulation, tremor was not present and so continuous motion was typically not present; rather the limb was held in place by low-force isotonic contractions, resulting in less beta-band desynchronization, which is likely the reason for the decreased performance during the prompted movement task. Indeed, classifier performance when stimulation was off was largely better than performance when stimulation was on for both subjects (data not shown), supporting this theory. It is important to note here that even though the classifiers for detecting movement and rest were trained under somewhat contrived conditions (prompted movement task), they were able to detect various kinds of movements tasks more akin to those experienced during everyday life with even better performance. This highlights the robustness of the system and its capability of functioning well during different kinds of movements, and suggests that it would perform well in everyday life.

For both the prompted movement task and the FTM drawing/writing tasks, the average stimulation voltage was less than the therapeutic value set by the clinician for continuous stimulation. Unsurprisingly, the average stimulation voltage was inversely correlated with the "stimulation label" sensitivity. While these two important metrics appear to be at odds with one another, increasing the specificity (true negative rate; i.e. how frequently rest is correctly classified as rest) of the system by improving classifier performance would act to decrease power consumption, but would not affect sensitivity. Therefore, increasing specificity is an important future step for improving the system. It is important to note that all power consumption has only been discussed in terms of the average stimulation voltage during a task, which is actually only a fraction of the power consumption from streaming data to and from the device. The reason for portraying data in this manner is that future iterations of the device will embed closed-loop capabilities onto the device itself, removing the power consumption due to telemetry from the equation.

For both subjects, the time between detecting the onset of a movement during the prompted movement task and the response of the system to increase stimulation was, on average, about 1.33 seconds. Ideally, this delay should be as small as possible so that symptoms are mitigated quickly. A large portion of this delay (at least 600 ms) comes from transmission delays between

the implanted device and external hardware. As mentioned above, future systems will circumvent this transmission time by using embedded algorithms to detect symptoms and trigger stimulation. While increasing the system's ability to respond quickly to movement is desirable, it may still be necessary to slowly ramp down stimulation when the system detects the cessation of movement. This slow decrease can mitigate some of the effects of false negatives.

The preceding discussion has evaluated the performance of the closed-loop system in the context of tremor-inducing movement detection, system delays and the correct delivery of stimulation. A related, and more important performance metric for a closed-loop DBS system is its therapeutic effect, that is, it's ability to mitigate the symptoms of the disease that afflicts the DBS user. To examine this, the ET subjects underwent the FTM tremor assessment under different stimulation conditions and their performance on the test was rated by blinded clinicians. For both subjects, scores were lowest during closed-loop DBS (compared to both off-stimulation and continuous stimulation at the therapeutic level). This is in agreement with the only other published closed-loop DBS study using neural activity as a control signal, which also saw closed-loop DBS being more therapeutically effective than continuous stimulation [6].

The most consistent improvements in scores across subjects were in right body side movements and left body side movements. During movements made with the right-side extremities, stimulation was typically on at some voltage much of the time, and thus average stimulation voltages were close to the therapeutic level. However, occasional false negatives from the classifiers meant that stimulation often ramped between the maximum therapeutic voltage and a lower voltage, but rarely turned off entirely. Similarly for left body side movements, stimulation was often on and ramping up and down, although the average voltages during left body movements were less than those for right body movements. It is possible that this intermittency of stimulation is somehow more therapeutically efficacious for treating ET; Little, et al, showed that random stimulation did not exert as much of a therapeutic effect as closed-loop DBS on continuous DBS in PD subjects, but also suggested that intermittent stimulation might be useful when delivered at the correct time [6]. The improvement in left-body (ipsilateral to DBS electrode) scores during CL-DBS is in agreement with what has been seen in prior literature, where there has been improvement in ipsilateral scores in ET during DBS [8]. However, confusingly, ipsilateral symptoms were slightly worse in S1 and only slightly improved in S2 with continuous stimulation, compared to off-stimulation. However, some aspect of the closed-loop stimulation, whether a lower average stimulation voltage or the frequent ramping of stimulation

voltage, appears to improve ipsilateral symptoms.

Tremor amplitude during the prompted movement task was also used to evaluate the therapeutic effect of the system. For subject S1, closed-loop and continuous stimulation both significantly decreased average tremor amplitude, as expected. For subject S2, however, average tremor amplitude was not significantly affected by stimulation condition. Both the disease symptoms and therapeutic effect of DBS for this subject were not as predictable as for subject S1, and could be caused by several factors. As mentioned in the Methods section, subject S2 was using medication to treat his symptoms, which may have had the effect of compressing the range of his symptoms, so that DBS did not exert as much of a therapeutic effect on tremor amplitude. So for both subjects, closed-loop control was at least as effective, if not more effective, at treating the symptoms of ET as continuous stimulation.

4.5 Summary

The aim of the work presented in this chapter was to develop and test a closed-loop DBS system for the treatment of ET. Cortical signals were used a biosignal for controlling stimulation, and machine learning was used to develop subject-specific models relating neural activity and tremor-inducing movement. These models were used in real time to detect movement and augment stimulation. This system delivered stimulation approximately 83-96% of the time that movement was occurring during a prompted movement task, and 100% of the time that movement was occurring during drawing and writing tasks. Also, therapeutically, closed-loop DBS was as effective, if not more effective, at mitigating the symptoms of ET as continuous stimulation.

References

[1] E. Bakstein, J. Burgess, K. Warwick, V. Ruiz, T. Aziz, and J. Stein, "Parkinsonian tremor identification with multiple local field potential feature classification.," *Journal of neuroscience methods*, vol. 209, no. 2, pp. 320–30, Aug. 2012.

[2] E. Bakstein, K. Warwick, J. Burgess, O. Stavdahl, and T. Aziz, "Features for detection of Parkinson's disease tremor from local field potentials of the subthalamic nucleus," *2010 IEEE 9th International Conference on Cyberntic Intelligent Systems*, pp. 1–6, Sep. 2010.

[3] C. Camara, P. Isasi, K. Warwick, V. Ruiz, T. Aziz, J. Stein, and E. Bakštein, "Resting tremor classification and detection in Parkinson's disease patients," *Biomedical Signal Processing and Control*, vol. 16, pp. 88–97, Feb. 2015.

[4] S. Fahn, E. Tolosa, and C. Marin, "Clinical rating scale for tremor," *Parkinson's disease and movement disorders*, pp. 271–280, 1993.

[5] J. A. Herron, M. C. Thompson, T. Brown, H. J. Chizeck, J. G. Ojemann, and A. L. Ko, "Chronic electrocorticography for sensing movement intention and closed-loop deep brain stimulation with wearable sensors in an essential tremor patient," *Journal of Neurosurgery*, pp. 1–8, 2016.

[6] S. Little, A. Pogosyan, S. Neal, B. Zavala, L. Zrinzo, M. Hariz, T. Foltynie, P. Limousin, K. Ashkan, J. FitzGerald, A. L. Green, T. Z. Aziz, and P. Brown, "Adaptive deep brain stimulation in advanced Parkinson disease.," *Annals of neurology*, vol. 74, no. 3, pp. 449–57, 2013.

[7] S. Pan, S. Iplikci, K. Warwick, and T. Z. Aziz, "Parkinson's Disease tremor classification – A comparison between Support Vector Machines and neural networks," *Expert Systems with Applications*, vol. 39, no. 12, pp. 10 764–10 771, Sep. 2012.

[8] Z. Peng-Chen, T. Morishita, D. Vaillancourt, C. Favilla, K. D. Foote, M. S. Okun, and A. W. Shukla, "Unilateral thalamic deep brain stimulation in essential tremor demonstrates long-term ipsilateral effects," *Parkinsonism & related disorders*, vol. 19, no. 12, pp. 1113–1117, 2013.

[9] D. Wu, K. Warwick, Z. Ma, M. N. Gasson, J. G. Burgess, S. Pan, and T. Z. Aziz, "Prediction of Parkinson's disease tremor onset using a radial basis function neural network based on particle swarm optimization.," *International journal of neural systems*, vol. 20, no. 2, pp. 109–16, Apr. 2010.

Chapter 5

Conclusion

Closed-loop deep brain stimulation (DBS) systems are a promising next iteration of DBS technology for the treatment of debilitating movement disorders. The purpose of this dissertation has been to contribute groundwork research demonstrating proof-of-concept for such closed-loop systems in the treatment of essential tremor (ET). The results herein will serve to inform and enable future work to to optimize closed-loop DBS systems, and consequently, augment the level of therapy received by the people who use this technology to improve the quality of their life.

5.1 Specific Aims

In the introduction to this thesis, several aims were set forth to guide the research being performed. These aims, and the work accomplished relating to each of them, consisted of the following:

Aim 1: Determine to what extent Parkinsonian and essential tremor can be detected from chronically-implanted DBS electrodes. The purpose of this aim was to examine symptom detection using the DBS electrode as a signal source to see if it would be usable in a closed-loop DBS system. To address this aim, signals were recorded from the DBS electrode implanted in the basal ganglia or thalamus of PD and ET patients, respectively, during tremor and tremor-free periods. Spectral analysis and machine learning were used to determine how well tremor can be detected using the network activity recorded from deep brain structures. For most subjects in both PD and ET patient populations, binomial classifiers were unable to satisfactorily detect tremor or tremor-inducing movements, typically resulting in accuracies

around 60-70%. Additionally, to examine long-term symptom detection, classifiers were trained on data from one visit, and then used to detect symptoms in subsequent visits. Again, for most patients detection was unsatisfactory. Also, because of the large artifacts present when DBS therapy was engaged, symptom detection during stimulation was not feasible.

Aim 2: Determine to what extent essential tremor can be detected from chronically implanted cortical electrodes. Because symptom detection using DBS electrodes was so poor, it was necessary to look for an additional signal source. Therefore, the purpose of this aim was to use a cortical electrode as a signal source to see if it would be improve symptom detection compared to the DBS electrode and thus be usable in a closed-loop DBS system. To address this aim, signals were recorded from an electrocorticography (ECoG) electrode implanted over the hand/arm region of M1/S1 in two ET patients. Again, spectral analysis and machine learning were used to examine how well tremor-inducing movement could be detected from these neural signals. For both subjects, tremor detection was much better than when using deep brain signals; accuracies were between 83-95%. Furthermore, tremor detection was also possible when stimulation was engaged, and classifiers were accurate between 63-95% of the time. Again, long-term detection was also examined; tremor detection using an initial visit to train classifiers up 8 months later also yielded high accuracies. These results showed that cortical signals yielded much better tremor detection than deep brain signals, and that cortical signals would be usable as a control signals for a closed-loop DBS system.

Aim 3: Develop and test the performance of a neural biofeedback signal, closed-loop system for mitigating essential tremor. After determining that cortical signals were better for tremor-inducing movement detection in ET, the purpose of this aim was to examine the performance of a closed-loop system using neural activity from the cortex as a control signal. The closed-loop system used a pair of binomial classifiers, one for off-stimulation and one for on-stimulation, to detect tremor-inducing movement from cortical signals and alter stimulation parameters in real-time. This system was tested in two ET subjects, and performance, both in terms of symptom detection and therapuetic effect, was quantified. The classifiers were able to detect tremor-inducing movement around 70% of the time, but stimulation was delivered around 85-95% of the time that subjects were moving in a prompted movement task. Detection was even higher during a drawing/writing task. For both subjects, the therapeutic effect of the closed-loop DBS was as good as, if not better than continuous DBS.

5.2 Future Work

Despite the work that has been accomplished herein, there still remains much to be done to improve closed-loop DBS therapy in order for it to achieve its maximal benefit for the people that use it. Many of these improvements will be enacted by the medical device companies designing, developing and manufacturing DBS technology, but critical research will be necessary to inform the choices made by these companies.

The experiments described in this thesis have focused on detecting arm and hand movements from neural signals. The cortical strip electrode implanted has a very small area of coverage, and because the subjects suffered from arm and hand tremor, it was placed to cover cortical areas relating to movement of these body parts. Tremor, however, can effect other parts of the body, such as as the head or legs. Additionally, detection of movements that don't evoke tremor but can be negatively affected by stimulation, such as walking and talking, might be desirable so as to turn stimulation off when they are occurring. Future iterations of DBS devices may permit implantation of multiple ECoG strip electrodes or grids of electrodes that could cover additional areas of cortex, such as lower body or head motor/somatosensory areas, or areas involved in speaking such as Broca's or Wernicke's areas. Also, the device used in these experiments was only capable of streaming data from a single channel; in the future, data could be streamed from all these areas simultaneously, monitoring normal and pathological behavior and then be used in more complex decision making algorithms for how to alter stimulation.

The main phenomenon seen in spectra during rest and movement in these experiments was beta-band (12-30 Hz) desynchronization (i.e. a drop in beta-band power during movement). This desynchronization is a spatially widespread occurrence that happens even in cortical areas corresponding to body parts that aren't actually moving [2]. So, the classifiers used in these experiments would likely detect movement from many different body parts. However, as described above, it may be desirable to turn stimulation off during some movements and back on during other movements. Using more electrodes that cover many different areas of cortex may allow for detection of much more localized increases in gamma-band (50-100 Hz) power during movement [2], and thus detection of distinct movements and more information for decision-making algorithms.

As alluded to above, the algorithms used for making decisions to alter stimulation parameters are a critical part of the system. In the experiments done in this dissertation, control decisions

were the simplest possible; if movement is detected, stimulation voltage is increased and vice versa if no movement is detected. An experiment was also done that required multiple negative classifier outputs to start decreasing voltage, but this algorithm only was only marginally more complicated. Furthermore, only stimulation voltage was ever altered, but other parameters, such as frequency, pulse width, electrode contacts and possibly even stimulation waveform could be altered in the future. Much work in the realm of control theory and perhaps artificial intelligence, as well as basic DBS research itself to better understand effects of changing different stimulation parameters, will have to be done to provide the optimal algorithms for making decisions in the closed-loop system. Another important parameter in future decision-making algorithms will be individual patient preferences. Just as symptoms can be different for different patients, even with same disease, so patient preferences regarding the trade-offs between therapeutic effect and side-effects can be different. It is conceivable that one DBS user would much prefer to never have side-effects but would tolerate some symptoms, while for another user this trade-off might be completely reversed. Also, these trade-offs will likely be context-specific, so allowing the user to modify their preferences in real-time will also be important.

In all of the closed-loop experiments presented in this thesis, the system was trained and tested during a single visit. Although results from chapter 3 suggest that training the system at one visit and then using it for an extended time (months or longer) may be feasible, this possibility has not been tested. Despite the stability of the cortical recordings seen in chapter 3, the neurodegenerative nature of ET and especially PD mean that symptoms typically worsen and/or spread over time [1][3]. So, even if the feedback signal is stable, the changing nature of the symptoms might mean that stimulation parameters need to updated periodically to alleviate symptoms. Future closed-loop systems may be able to incorporate external devices, such as commercial smartwatches, to continuously monitor the therapeutic effect of the system, and adjust parameters if necessary. With more electrodes, it also might be possible to directly monitor the efficacy of the system using neural signals, such as beta-band power for PD.

5.3 Significance of Work

The results outlined in the specific aims above are significant in several ways. First, they inform future iterations of closed-loop DBS devices regarding the best choice of signal source for detecting symptoms; at least for essential tremor, cortical activity is more useful than thalamic

activity. Second, they demonstrate long-term stability of cortical signals, which is exceedingly important for chronic closed-loop DBS use. Third, they demonstrate a closed-loop DBS system for mitigating the symptoms of ET that is novel in three ways: uses a cortical signal; senses from a chronically-implanted, commercially-available (even if currently investigational) device; and harnesses machine learning to build patient-specific models for symptom detection.

References

[1] S. Fahn, "Description of parkinson's disease as a clinical syndrome," *Annals of the New York Academy of Sciences*, vol. 991, no. 1, pp. 1–14, 2003.

[2] G. Pfurtscheller, B. Graimann, J. E. Huggins, S. P. Levine, and L. A. Schuh, "Spatiotemporal patterns of beta desynchronization and gamma synchronization in corticographic data during self-paced movement," *Clinical Neurophysiology*, vol. 114, pp. 1226–1236, 2003.

[3] J. D. Putzke, N. R. Whaley, Y. Baba, Z. K. Wszolek, and R. J. Uitti, "Essential tremor: predictors of disease progression in a clinical cohort.," *Journal of neurology, neurosurgery, and psychiatry*, vol. 77, no. 11, pp. 1235–1237, 2006.